


ARTICLE



Molecular Diagnostics

Anti-PEc: Development of a novel monoclonal antibody against prostate cancer

Athanasios Armakolas¹ , Nektarios Alevizopoulos^{1,6}, Martha Stathaki^{2,6}, Constantina Petraki³, George Agrogiannis⁴, Martina Samiotaki⁵, George Panayotou⁵, Eirini Chatzinikita¹ and Michael Koutsilieris¹

© The Author(s), under exclusive licence to Springer Nature Limited 2024

BACKGROUND: The Ec peptide (PEc) that defines the IGF-1Ec isoform, is associated with prostate cancer progression by inducing proliferation, metastases, and tumour repair. On these grounds, an anti-PEc monoclonal antibody (MAB) was developed. Our objective is to examine the effects of this antibody on prostate cancer and its possible side effects.

METHODS: The effects of the obtained MAB were examined in cancer and non-cancerous cell lines (unmodified and modified either to overexpress or silence PEc) and in tumours in SCID mice injected with unmodified prostate cancer cells. The investigation was obtained with respect to cellular proliferation, migration, invasion, toxicity to tumours, effects on the cell cycle, immune response activation, effects on mesenchymal stem cell mobilisation leading to tumour repair, tissue distribution, and toxicity to mice.

RESULTS: Anti-PEc MAB treatment led to a significant decrease in cellular proliferation, migration, and invasion compared to the untreated cell lines ($p < 0.0005$ in every case). Mechanistically, these effects were associated with the downregulation of pERK1/2 and vimentin and the upregulation of E-Cadherin. In vivo, anti-PEc MAB treatment was associated with a significant decrease in tumour size and metastases rate ($p < 0.0005$ in every case) by reversing the tumours mesenchymal phenotype. It also inhibited host stem cell mobilisation towards the tumour, leading to apoptosis. Anti-PEc MAB assessment in respect to distribution and toxicity, indicated its tumour specificity and lack of toxicity.

CONCLUSIONS: These data indicate that the therapeutic targeting of PEc with the anti-PEc MAB may have considerable clinical benefit for prostate cancer patients.

British Journal of Cancer (2024) 131:551–564; <https://doi.org/10.1038/s41416-024-02713-8>

INTRODUCTION

The role of IGF-1 in cancer is well-established [1, 2]. The *Igf-1* gene is transcribed and translated in humans in the form of multiple precursor IGF-1 polypeptides, namely isoforms. These are the IGF-1Ea the predominant form, IGF-1Eb, and IGF-1Ec, all of which undergo posttranslational modifications such as glycosylation and proteolytic cleavage, leading to the production of the mature IGF-1 (mIGF-1) [3, 4]. Till recently the role of the carboxy-terminal E peptides (PEa, PEb, and PEc) deriving from the cleavage of the pro-IGF-1 isoforms, was not known and at large still remains elusive [5, 6]. The Ec peptide, the part of the IGF-1Ec isoform that is cleaved prior to the production of the mIGF-1, has been associated with prostate cancer progression [7]. PEc overexpression in prostate cancer experimental models was associated with a significant increase in cellular proliferation and induction of the epithelial-to-mesenchymal transition (EMT) process, which has a fundamental role in the mechanism of cancer cell invasion and

metastasis. PEc effects are generated by activating the ERK 1/2 pathway, through an unknown receptor, other than IGF-1R, IR, or any of the IGF-1/IR hybrid receptors produced by the heterodimerization of the IR and IGF1R respective monomers [8, 9]. The oncogenic role of PEc was also verified by the fact that the introduction of PEc overexpressing cells (normal and cancer cell lines) subcutaneously and orthotopically in SCID mice, leads to a significant elevation of both growth and metastatic rates of the resulting tumours compared to the tumours obtained from the wild type (wt) cell lines [9]. Apart from its oncogenic effect, tumour-secreted PEc was also found to be associated with host mesenchymal cell mobilisation towards the tumour. The mobilisation of host MSC to the tumour has been associated to tumour repair [10].

Prostate cancer cell lines in in vitro conditions do not express the IGF-1Ec isoform. However, the tumours developed by the introduction of unmodified prostate cancer cells into SCID mice,

¹Physiology Laboratory, Medical School, National and Kapodestrian University of Athens, Athens, Greece. ²Surgical Department, Elena Venizelou Hospital, Athens, Greece. ³Department of Pathology, Metropolitan General Hospital, Athens, Greece. ⁴Department of Pathology, University of Athens, Medical School, National and Kapodestrian University of Athens, Athens, Greece. ⁵Bioinnovation Institute, Biomedical Science Research Center "Alexander Fleming.", Vari, Greece. ⁶These authors contributed equally: Nektarios Alevizopoulos, Martha Stathaki. ✉email: aarmakol@med.uoa.gr

expressed increasing amounts of IGF-1Ec as they progressed [10]. Recent evidence suggests that the mechanism leading to tumour PEC secretion is associated with the tumour-host immune cell-cell interaction [10]. Immune cells secrete IL-6 upon prostate cancer cellular interaction. IL-6, through the JAK2/STAT3 pathway, seems to be a key molecule regulating tumour *igf-1Ec* and *il6* genes transcription. Tumour IL-6, acting in an autocrine/paracrine mode of action, further induces IGF-1Ec expression in prostate cancer, consequently leading to the elevation of the PEC amount and tumour progression [10]. Consistent with the laboratory evidence is the fact that IGF1-Ec expression determined in human prostate cancer biopsies was found to be directly positively associated with tumour grade and stage [11, 12].

The fact that PEC secretion is central to tumour progression in prostate cancer (proliferation metastasis and repair), prompted us to proceed to test the effects of anti-PEC monoclonal antibodies in prostate cancer. The aim of this study is to develop a monoclonal antibody against the tumour-secreted PEC prior to abolishing its oncogenic effects, without affecting the IGF-1-IGF-1R axis. The major evidence obtained suggests that the introduction of the anti-PEC monoclonal antibody in *in vitro* and *in vivo* cancer models inhibits cellular proliferation, metastasis, and invasion in both androgen receptor-positive and androgen receptor-negative prostate cancer.

METHODS

Patients

Prostate tissues after tumour characterisation, were examined from 108 age-matched patients with prostate cancer, who had undergone radical prostatectomy. Inclusion criteria were: the presence of prostate cancer of any stage and patient's age (60 to 80). Exclusion criteria were: the absence of cancerous tissue at the paraffin sections and age > 80 years. Out of a total 108 patients eventually 100 were included in the study. A written informed consent (IC) was obtained from all the patients. The study has been approved by the Institutional Ethics Committee and all the experimental procedures conformed to the Declaration of Helsinki. These prostate tissue paraffin sections were analysed for PEC expression using the anti-PEC monoclonal antibody that has been further used in this study as a therapeutic agent.

Anti-PEC MAb production. One hundred and twenty different monoclonal antibodies were produced using the hybridoma technique (Absea Biotechnology Ltd, Haidian district Beijing 100,085 China). Briefly, five mice were immunised with the human PEC or scrambled peptide (prior to the development of a valid isotype-matching control antibody). Spleen cells were fused with immortal myeloma cells. The obtained monoclonal antibodies were tested for specificity and sensitivity against the antigen of interest (human PEC: NH2-YQPPSTNKNTKSQRRKGSTFEERK) by an in-house ELISA method. Different concentrations of each antibody ranging from 0–1000 ng/ml were added in wells coated either with human PEC, mouse PEC or with the scrambled peptide (1 µg/ml). Ten different monoclonal antibodies were selected for their specificity and sensitivity against human (and mouse) PEC and they were further tested by dot blot analysis. The scrambled peptide (CSKNKTSREGTKFSEKYRPNTRPQ) was used as a negative control. The most potent anti-PEC monoclonal antibody was selected. DNA coding for the aa sequence of this MAb was synthesised and cloned into the mammalian transient expression vector PETE V2 (Fusion Antibodies Pembroke Loop Road, Belfast Ireland). The MAb was expressed using CHO based transient expression system and the resulting antibody containing cell culture supernatants was clarified by centrifugation and filtration. MAb purification was obtained using AKTA affinity chromatography. The purified antibody was dialysed into PBS. The purity of the MAb was determined to be >95% (reducing and denaturing SDS PAGE and size exclusion chromatography, fig S1). MAb concentration was determined by measuring the absorbance at 280 nm calculated using the standard extinction coefficient $205,000 \text{ M}^{-1} \text{ cm}^{-1}$ (or $1.0 \text{ mg/mL} = A_{280}$ of 1.37, assuming a MW = 150,000 Da).

Binding analysis

Binding assays were performed by first capturing the IgG MAb by using an anti-mouse Fc Octet. The MAb capture biosensors were then submerged in

wells containing 300 nM of antigen. Steps were performed at 25°C at a constant flow rate of 1000 rpm. Dissociation rate constants (KD) were estimated using the Forte Bio data analysis software (Fusion Antibodies Pembroke Loop Road, Belfast Ireland). Due to the small size of the antigen (24aa) Octet binding analysis did not work. Therefore, binding analysis was carried out by a dot blot assay against different PEC fragments (aa: 1-12, 13-24, 1-6, 7-12, 13-19, 20-24, and against the whole PEC. Briefly, different concentrations of each fragment (10, 20, 40, 80 ng/mL) were applied onto a nitrocellulose strip, after drying the membrane was blocked by 5% BSA for 1 hour and then incubated with 2.5 µg/mL of the anti-PEC MAb for 1 h at RT. After washing the membrane was incubated with an anti-mouse HRP antibody (1:2,000 dilution); (Santa Cruz Biotechnology). Visualisation took place by exposing the blots to x-ray film after incubation with freshly made ECL substrate for 3 min (SuperSignal, Pierce Biotechnology, Rockford, IL, USA).

ELISA

Wells of a microplate were coated with different concentrations of the synthetic PEC (0 to 1 µg/mL). After washing the excess media, administration of a custom-made rabbit anti-human polyclonal anti-PEC antibody (1/5000) or the newly made anti-PEC MAb at different concentrations followed (1-10 µg/ml). Detection was carried out with a horseradish peroxidase-conjugated goat anti-rabbit antibody at 1:1,000 dilution (Thermo Scientific [Thermo Fisher Scientific Inc., Waltham, MA, USA]). As a substrate, we used TMB. The reaction was stopped with 2 mol/L sulphuric acid. The absorption of the plate was measured within 20 min at 450 nm and 540 nm as a reference, using a microplate reader (VersaMax, Molecular Devices, Sunnyvale, CA, USA).

Competition assay

Wells of a microplate were coated with 1 µg/ml of synthetic PEC. After washing anti-PEC MAb was introduced in each well (5 µg/ml) together with PEC peptide at different concentrations/well (0.2, 0.4, 0.6, 0.8, 1, µg/ml). As a negative control, we used human serum from 3 different individuals. Detection was carried out with a horseradish peroxidase-conjugated goat anti-rabbit antibody at 1:1,000 dilution (Thermo Scientific [Thermo Fisher Scientific Inc., Waltham, MA, USA]). As a substrate, we used TMB. The reaction was stopped by administering 2 mol/L sulphuric acid solution. The absorption of the plate was measured within 20 min at 450 nm and 540 nm as a reference using a microplate reader (VersaMax, Molecular Devices, Sunnyvale, CA, USA).

Cell cultures

Cell lines. Early passage (<10) wild type PC-3 cells (wtPC-3), an androgen resistant, p53-negative and Kirsten-Ras (K-Ras) mutated human prostate cancer cell line, DU-145 in nude mice; forms adenocarcinomas (grade II) that are not detectably hormone-sensitive, MCF-7 a breast cancer cell line and DLD-1 a colorectal adenocarcinoma cell line [13], were obtained from American Type Cell Culture (ATCC, Bethesda, MD, USA). Authentication of these cell lines was not obtained since they were all newly acquired (less than 1 month before the experiments). PC-3, DU-145, and MCF-7 cells were maintained in Dulbecco-modified Eagle medium, and DLD-1 cells were maintained in RPMI media (Cambrex, Walkerville, MD, USA), supplemented with 10% heat-inactivated foetal bovine serum (FBS) (Biochrom, Berlin, Germany) at 37 °C in a humidified atmosphere of 5% CO₂.

Stable siRNA KD

IGF-1Ec PEC was silenced in wtPC-3 cells by stable siRNA transfection using the psiRNAh7SKneo G1 kit (Sigma-Aldrich) according to the manufacturer's instructions. Complementary oligonucleotides compatible with BbsI restriction enzyme prior to their insertion into the psiRNA-h7SKneo vector were designed using the siRNA Wizard software (www.sirnawizard.com). The oligonucleotides used were these: forward: ACCTCGAGAA GGAAAG-GAAG TACATTCAA GAGAAT GTAC TTCCTTCTCT TCTCTT; and reverse: CAAAAGAGAGA AGGAAAGGA AGTACATTCT CTTGAAATGT ACTTCCTTCTCTCG. The siRNA insertion was confirmed by enzyme digest with SpeI and by bidirectional sequencing using the primers provided by the kit (forward OL559 and reverse OL408).

Cell proliferation MTT assay

Wt and modified PC-3 and DU-145 cells were plated at a cell density of 750 cells/well in 96-well plates and grown with DMEM containing 10% FBS.

After 24 and 48 h, the cells were cultivated with 10% MTT as described previously [9, 14]. MTT assays measure mainly the metabolic activity of cells in culture, indirectly associated with cell viability status. Trypan blue exclusion assays. PC-3 and DU-145 cells were plated at a cell density of 3.5×10^4 cells/well in 6-well plates and grown with DMEM containing 10% FBS. After 24 h and 48 h of seeding cells, the cell number was counted as described previously.

Western Blot analyses

The cell extracts were obtained by lysis in RIPA buffer (50 mmol/L Tris-HCl, 150 mmol/L NaCl, Sigma-Aldrich) containing 0.55 Nonidet P-40, protease 1 mmol/L phenylmethylsulfonyl fluoride (PMSF) (Sigma-Aldrich), 10 µg/mL aprotinin, 10 µg/mL leupeptin; (SigmaAldrich) and phosphatase inhibitors (1 mmol/L sodium orthovanadate, 1 mmol/L NaF) (Sigma-Aldrich). After 30 min incubation on ice, the lysates were cleared by centrifugation (19,722 g) (15 min, and 4 °C). Protein concentrations were determined by Bio-Rad Protein Assay (Bio-Rad Laboratories RRID:SCR_008426, Hercules, CA, USA). Equal amounts of cell lysates (20 µg) were heated at 95 °C for 5 min, electrophoresed on 12% SDS-PAGE under denaturing conditions, and transferred onto nitrocellulose membrane (Bio-Rad Laboratories). The blots were blocked with TBS-T (20 mmol/L Tris-HCl [pH 7.6], 137 mmol/L NaCl, and 0.1% Tween 20) containing 5% non-fat dried milk at room temperature for 1 h. The membranes were probed overnight with primary antibodies. The primary antibodies used were: rabbit anti-phospho and total ERK1/2 and rabbit anti-phospho and total Akt (1:1,000), (all from Cell Signalling Technology Inc., Danvers, MA, USA); rabbit anti-glyceraldehyde 3-phosphate dehydrogenase (anti-GAPDH), The blots were washed and incubated with a secondary goat antibody raised against rabbit IgG conjugated to horseradish peroxidase (1:2,000 dilution); (Santa Cruz Biotechnology). The bands were visualised by exposing the blots to x-ray film after incubation with freshly made ECL substrate for 3 min (Super-Signal, Pierce Biotechnology, Rockford, IL, USA).

Quantitative real-time PCR (qRT-PCR)

Total RNA was isolated using TRIzol (Invitrogen [Thermo Fisher Scientific]). Quantitative real-time PCR was performed in the Bio-Rad iQ5 multicolour real-time PCR detection system, using SYBR Green Supermix (Bio-Rad Laboratories). Each reaction was performed in triplicate and values were normalised to GAPDH. Primers:

PEC: Fwd 5'-TATCAGCCCCCTACCA-3',
Rvs 5'-CTTGCGTTCTCAATGTAATTCCT-3'

E-cadherin: Fwd 5'-TGGAGGAATCTTGCTTTC-3',
Rvs: 5'-CGTACATGTCAGCCAGCTTC-3'

Vimentin: Fwd 5'-GACAATGCGTCTCTGGCAGCTCT-3',
Rvs 5'-TCCTCCGCTCCTGCAGTTCT-3',

Ki-67: Fwd 5-GAAAGAGTGGAACCTGCCCTC-3,
Rvs: 5-GACCAAGTTTACTACATCTGCC-3.

Effect of the anti-Pec MAb on prostate cancer cell lines

Apoptosis detection: An Annexin V-FITC Apoptosis Detection kit was used to study the effect of anti-Pec MAb on apoptosis. Samples were prepared according to the manufacturer's instructions. Briefly, Cancer and normal cells were seeded in 6-well plates at a density of about 2×10^5 cells/well in 1 ml growth medium. The cells were then co-incubated either with human serum with and without MAb, with PBMCs, and with serum and PBMCs for 24 h. The cells were collected, washed twice with PBS, resuspended in 1X binding buffer (cat. no. B9796, Sigma-Aldrich; Merck KGaA), and stained with Annexin V-FITC conjugate (cat. no. A9210, Sigma-Aldrich, ~50 µg/ml in 50 mM Tris-HCl, pH 7.5, containing 100 mM NaCl) and propidium iodide (PI; cat. no. P2667; Sigma-Aldrich; Merck KGaA; 100 µg/ml in 10 mM potassium phosphate buffer, pH 7.4, containing 150 mM NaCl) for 10 min at room temperature in the dark. Subsequently, the samples were quantified by a flow cytometer (CyFlow Space; Sysmex Partec GmbH) and analysed by FloMax cell cycle analysis software, version 2.82 (Quantum Analysis GmbH).

Cell cycle analysis: Cell cycle analysis was performed using a DNA content quantitation assay kit (Nanjing KeyGen Biotech Co., Ltd.). The cells were seeded in a 6-well plate at a density of 5×10^5 cells/well in 1 ml RPMI-1640 growth medium and treated with linalool (2.5 mM) for 24 h at 37 °C. After the treatment, the cells were collected and fixed with 70% ethanol at 4 °C overnight. The cells were washed 3 times with PBS and stained with PI in the presence of 1% DNase-free RNase A at 37 °C for

30 min prior to flow cytometry analysis. The distribution of cells among the different cell cycle phases was determined using FloMax cell cycle analysis software, version 2.82 (Quantum Analysis GmbH).

Determination of the cytotoxic effect of the anti-PEC MAb: Prior to determining if the effects of the anti-Pec MAb on cancer cells are associated with complement-dependent cytotoxicity 200 µL of human serum collected from 5 healthy individuals were added to the test wells.

The effect of the antibody-dependent cellular cytotoxicity that may be induced by our MAb in prostate cancer cells was determined by the administration of 200 µL at a density of about 500,000 cells (1/10 ratio). After 24 h incubation that led to the induction of expression of PEC from the cancer cells, anti-Pec MAb or an anti-human IgG isotype control was administered at a dose of 0.5 mg/ml. The cells were collected and analysed at 12 hours and measured.

The complement-dependent cellular cytotoxicity was examined by co-incubating human PBMCs and autologous serum from each volunteer with cancer cells. After a 24 hr incubation, the anti-Pec MAb or the isotypic control antibody was added and the cells were collected and analysed at 12 hours.

In every case where cancer or normal cells were co-incubated with PBMCs, PBMCs were removed by using CD45-coated dynabeads (Thermo Fisher Scientific) according to the manufacturer's instructions. Briefly, dynabeads were added in a cell suspension containing all the cells (shaking) and were allowed to interact with the CD45 positive cells for 20 min (r.t), then the bead-bound cells were separated by using a magnet. The rest of the cells were kept for further analysis.

Immunofluorescence Staining: Cultured cells on chamber slides were stained by an indirect immunofluorescence method. Cells were rinsed in PBS and fixed with ice-cold 80% methanol for 10 min at room temperature. They were permeabilized with PBS plus 0.5% Triton X-100 (Sigma Aldrich) for 10 min. They were then incubated with primary antibodies overnight at 4 °C: rabbit anti-E-cadherin (1:100, Abcam) or mouse anti-Pec MAb (1:1,000) or mouse anti-vimentin (1:100, Abcam) in PBS. After three washes with PBS, 5 min at room temperature, cells were incubated for 30 min with goat anti-rabbit IgG conjugated to the fluorescent Alexa 488 dye (1:2,000, Abcam) or with goat anti-mouse IgG conjugated to the fluorescent Alexa 555 dye (1:2,000, Abcam) in PBS. After three washes, samples were stained with DAPI (1 µg/mL) for viewing with the microscope (Olympus BX40; Olympus Corporation, Tokyo, Japan).

Cell migration and invasion were analysed using Cultrex cell invasion assay (Trevigen Inc. Gaithersburg, MD, US) according to the manufacturer's instructions. Briefly, for the invasion assay, the membrane in the upper chamber of the 96-well plate was coated with 0.5 × basement membrane matrix/Matrigel. For the migration assay, the membrane was left uncoated. Mesenchymal stem cells were starved in the serum-free medium for 8 hours prior to the assay, then seeded at a density of 5×10^4 /well. 24 h after seeding, the cells on the lower surface were dissociated and counted.

Subcutaneous injections in male SCID mice. SCID mice (6 weeks old) (total $n = 140$) were obtained from Democretos Laboratory, Greece. In each case, the number of experimental animals required was based on a power analysis based on results obtained from previous studies obtained in our Laboratory. Mouse handling and experimental procedures were approved by the Hellenic Ministry of Rural Development and Food, General Directorate of Veterinary. Animal handling and experimental procedures were obtained in the Experimental Surgery Laboratory of the Athens Medical School. Implantations were carried out as previously described [7]. Briefly, a suspension of 5×10^6 cells in 200 µL in 1× PBS was injected subcutaneously in each mouse. The mice were injected with tumour cells when were 12 weeks old and they were separated into four different groups/tumour.

Determination of the optimum MAb concentration for prostate cancer treatment was obtained by testing different concentrations of the anti-Pec MAb. The concentrations used were 5, 10 and 20 mg/kg, three times/week. Prior to determining the optimum number of SCID mice per case, we carried out a power analysis using the mice tested to determine the optimum concentration (5/case).

Randomly selected groups were administered with the anti-Pec MAb and the other groups were administered with an isotype control. Stratified randomisation was used to separate these mice and different researchers measured the tumours in each case. In the case of prostate cancer xenografts, we used male mice, in the case of breast cancer xenografts we

used female mice and in the case of colon cancer xenografts, we used an equally mixed population. In every case, the allocation of the cages with the mice (5/ cage), as well as the MAb administration (anti-PEC or isotype), were obtained by a technician who was not directly involved in the project. Tumour volume was estimated blindly by measuring the three tumour dimensions by calliper. Data collection and tumour analysis were carried out by independent researchers. Inclusion criteria were the development of palpable tumours and the good health of mice according to the Severity Assessment Framework of the European Commission. Exclusion criteria were set as the lack of tumour development after cancer cell injection and tumour development of more than 1.5 cm³. The size limitation of any single tumour in a mouse is 2.0 cm in diameter, according to the instructions provided by the Hellenic Ministry of Rural Development and Food, General Directorate of Veterinary. In our study, tumours did not exceed the 2 cm in diameter limit in any case, according to the limitations

IF and FISH in paraffin sections

FISH was carried out according to the manufacturer's instructions (Cambio Ltd, The Irwin Centre, Scotland Road, Dry Drayton, Cambridge, UK). Briefly, slides were deparaffinized in xylene and dehydrated in a sequential series of ethanol baths (100%, 96%, 80%, 70%). Slides were then treated with Pepsin solution (ZytoVision GmbH Fischkai 1D-27572 Bremerhaven Germany) and post-fix in paraformaldehyde solution took place for 2 min. 10 µl of ready-to-use paint mix was applied at the centre of the slide (Cambio Starfish Pan Centromeric Chromosome Paint 1697-MC3-01) together with FITC labelled anti mouse CD45 (1:500), (cat. # 12-0461-80, Thermo Fisher Scientific, Bonn, Germany). The slides were then denatured at 60 °C for 10 min and hybridised at 37 °C overnight. After washing in formamide and detergent wash solution the slides were incubated with DAPI (Life Technologies) for 5 min at room temperature and they were then covered with Fluorescence Mounting Media (DAKO. 2966 Industrial Row Troy, Michigan 48084, USA). A total of 10 sections were analysed per tumour ($n = 10$ /case). Visualisation took place using a microscope (Olympus BX40, Tokyo, Japan), and the software used was the Case Data Manager 5.5 (Applied Spectral Imaging, Inc. 5315 Avenida Encinas, Suite 150 Carlsbad, CA 92008, USA

Apoptosis in xenograft tumours

To detect apoptotic cell death in xenograft tumours, the terminal deoxynucleotidyl transferase dUTP nick end labelling (TUNEL) assay was performed using the in situ TUNEL cell apoptosis detection kit (KGA702, KeyGEN BioTECH). Slides were prepared according to the manufacturer's instructions. Three fields of each section were visualised (400× magnification). The immunosignal indices were calculated as follows: (Apoptotic cell number/total cell number) × 100.

Immunohistochemistry

Formaldehyde-fixed cancer samples were paraffin wax embedded and processed for paraffin sections. Microtome sections of 3 µm were allowed to adhere to glass slides, dried at 37 °C overnight, dewaxed in xylene, and rehydrated in serial dilutions of ethanol. The sections were then incubated with the same primary antibody used for the Western blot analyses, that is, the polyclonal anti-IGF-1Ec antibody at a dilution of 1:1000 in PBS overnight at 4 °C. Secondary biotinylated goat anti-rabbit IgG antibody (Dako Real EnVision; Dako Glostrup, Denmark) was then added and tissue sections were visualised under light microscopy (Nikon Eclipse 80i; Nikon, Tokyo, Japan), while negative control staining procedures were also included in all immunohistochemical analyses as described elsewhere [3]. Samples were photographed using a digital camera (Nikon DS-2 MW; Nikon). Image analysis was performed in six random fields from each slide using the Image Pro Plus 5.1 software (Media Cybernetics, Bethesda, MD, USA). IGF-1Ec (brown staining) average intensity levels, measured using arbitrary units on a linear scale from 0 (representing black) to 255 (representing white), and the average percentage of the extent of brown staining are combined in the following equation: IGF-1Ec expression = 255 – average intensity levels of brown staining × average percentage of the extent of brown staining. The mean intensity and extent of levels of brown staining for the six representative optical fields were estimated in each case and compared.

Proteomics/Phosphoproteomics. Proteomic sample preparation using the single-pot, solid-phase-enhanced sample preparation Sp3-mediated protein digestion protocol:

The PC3 WT cells were subjected to PEC and Mab treatments, in four biological replicas, washed with ice-cold PBS, and finally lysed in lysis buffer consisting of 4% SDS, 0.1 M DTT, and 0.1 M Tris pH 7.4. The samples were subjected to heating for 3 min at 99 °C followed by a centrifugation step for 15 min at 17 000 × *g*. The supernatant was collected and processed according to the Sp3 protocol^(Hughes) including an alkylation step in the dark for 15 min in 10 mg/ml iodoacetamide (Acros Organics). 20 µg of beads (1:1 mixture of hydrophilic and hydrophobic SeraMag carboxylate-modified beads, GE Life Sciences) were added to each sample in 50% ethanol. The proteins were allowed to bind to the beads for 15 min followed by repeated steps of protein clean-up using a magnetic rack. The beads were washed two times with 80% ethanol and once with 100% acetonitrile (Fisher Chemical). The captured beads proteins were digested overnight at 37 °C under vigorous shaking (1200 rpm, Eppendorf Thermomixer) with 1 µg Trypsin/LysC (MS grade, Promega) prepared in 100 mM TEAB. The next day, the supernatants were collected and the peptides were purified using a modified Sp3 clean-up protocol and finally solubilized in the mobile phase A (0.1% formic acid in water), sonicated, and the peptide concentration was determined through absorbance at 280 nm measurement using a nanodrop instrument.

Phosphopeptide enrichment was performed according to the instructions of the High-Select TiO₂ phosphopeptide enrichment kit (Thermo Scientific, A32993) using spin columns. The eluted peptides were dried down and solubilized in Buffer A.

LC-MS/MS analysis: Samples were run on a liquid chromatography-tandem mass spectrometry (LC-MS/MS) setup consisting of a Dionex UltimateRSLC online with a Thermo Q Exactive HF-X Orbitrap mass spectrometer (Thermo Scientific). Peptidic samples were directly injected and separated on a 25 cm-long analytical C18 column (PepSep, 1.9 µm₃ beads, 75 µm ID, Bruker) using a one-hour long run, starting with a gradient consisting of 7% Buffer B (0.1% Formic acid in 80% Acetonitrile) to 35% for 40 min and followed by an increase to 45% in 5 min and a second increase to 99% in 0.5 min and then kept constant for equilibration for 14.5 min. The flow rate was set to 400 nl/min in the sample loading phase and lowered to 250 nl/min in the main phase of sample analysis. A full MS was acquired in profile and positive mode using the mass spectrometer, operating in the scan range of 375–400 *m/z* using 120 K resolving power with an AGC of 3 × 10⁶ and max IT of 60 ms followed by data independent analysis using 8 Th windows (39 loop counts) with 15 K resolving power with an AGC of 3 × 10⁵ and max IT of 22 ms and normalised collision energy (NCE) of 26. At least two technical replicas were acquired per sample.

Data Analysis: Orbitrap raw data was analysed in DIA-NN 1.8.1 (Data-Independent Acquisition by Neural Networks)^(Demichev) through searching against the Human UniProt database containing 20578 proteins (one protein per gene, UP000005640_9606) using the library-free mode of the software and allowing up to two tryptic missed cleavages. A spectral library was created from the DIA runs and used to reanalyse them. DIA-NN default settings have been used with cysteine carbamidomethylation enabled as a fixed modification. Phosphorylation of serines, threonines, and tyrosines (STY) was set as variable modification. The match between runs (MBR) feature was used for all analyses the output (precursor) was filtered at 0.01 FDR and finally, the protein inference was performed on the level of genes using only proteotypic peptides. The generated results were processed statistically and visualised in the Perseus software (1.6.15.0)^(Tyanova).

Deposition: The mass spectrometry proteomics data have been deposited to the ProteomeXchange Consortium via the PRIDE (Perez-Riverol et al., 2019) partner repository with the dataset identifier.

Statistical analysis

The results obtained by the trypan blue and MTT analyses were assessed by the two-tailed equal variance Student *t* test (SPSS v. 11 statistical package; SPSS RRID:SCR_002865, [IBM, Armonk, NY, USA]). Statistical significance was set at *p* values less than 0.05 ($p < 0.05$). The results obtained from the prostate cancer patients' tumours were analysed by the Kolmogorov-Smirnov test for analysis of variance in all continuous variables, the Kruskal Wallis test, and Independent-Samples Mann-Whitney *U* Test. The choice of methods for statistical testing of continuous variables was based on whether the data permitted parametric or nonparametric analysis. Comparisons of IGF-1Ec, E-Cadherin, Vimentin, and Ki-67 expression, between groups, were accordingly performed using Student *t* test. A *p*-value < 0.05 was considered statistically significant.

The proteomics data were processed in Perseus 1.6.15.0 (Tyanova). Values were log [2] transformed, a threshold of —% of valid values in at least one group was applied and the missing values were replaced from the normal distribution. For statistical analysis, Student's t-test was performed and permutation-based FDR was calculated.

Study approval. A written informed consent (IC) was obtained from all the patients prior to participation in the present study. The study has been approved by the Institutional Ethics Committee and all the experimental procedures conformed to the Declaration of Helsinki

RESULTS

Antibody characterisation

The DNA coding for the a.a sequence of this MAb was synthesised and cloned into the mammalian transient expression vector PETE V2 (Fusion Antibodies Pembroke Loop Road, Belfast Ireland). The MAb was expressed using CHO based transient expression system. The resulting antibody containing cell culture supernatants was clarified by centrifugation and filtration. The purity of the MAb was determined to be >95% (reducing and denaturing SDS PAGE and size exclusion chromatography where the chromatogram shows

one major peak (>95% total area), (fig S1a and b respectively). MAb concentration was determined by measuring the absorbance at 280 nm calculated using the standard extinction coefficient $205,000 \text{ M}^{-1} \text{ cm}^{-1}$ (or $1.0 \text{ mg/mL} = \text{A}280$ of 1,37, assuming a $\text{MW} = 150,000 \text{ Da}$). The specificity and sensitivity of the selected anti-PEC, MAb were examined by dot blot analysis against different human PEC fragments and against the whole mouse PEC (determine its eligibility for use in toxicity assays conducted in mice). Anti-PEC MAb recognised the human full-length PEC (1-24 aa) and the second half (13-24 aa) (Fig. S1c). The aforementioned MAb also recognises the full-length mouse PEC (Fig. S1c). ELISA analysis using as an antigen the synthetically formed PEC at different concentrations as well as a competition assay where in the already PEC coated wells of the ELISA plate, PEC was gradually introduced together with the anti-PEC MAb, indicated that the present anti-PEC MAb presented similar specificity and sensitivity to the polyclonal anti-PEC (Fig. S1d, e). In order to obtain naturally produced PEC from cancer cells, we used a previously described model, where co-incubation of cancer cells with cells of the immune system (PBMCs) induces PEC secretion by cancer cells (Fig. S1d) [12].

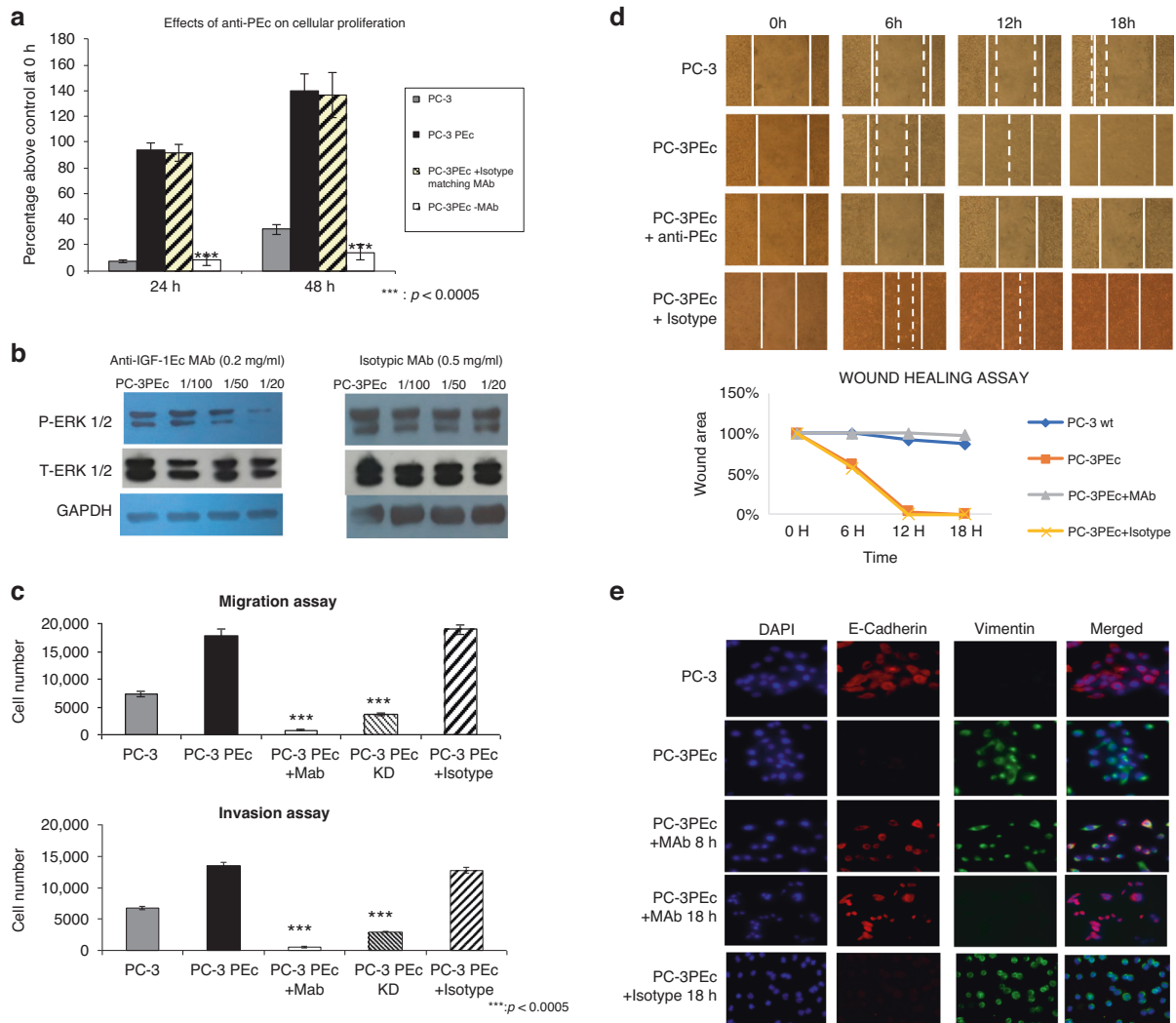


Fig. 1 In vitro analysis of the effects of anti-PEC MAb. **a** Proliferation assay indicating the inhibition of cellular proliferation of PEC overexpressing prostate cancer cell lines. **b** WB analysis where the downregulation of proliferation in anti-PEC MAb treated cell lines is associated with a decrease of the PERK 1/2 levels. **(c)** Migration and invasion assays. Treatment of both prostate cancer cell lines is associated with a significant inhibition of migration and invasion rates. **d** Wound healing assay treatment of the prostate cancer cell lines is associated with a significant inhibition of cellular migration starting from the 6th hour. **e** Treatment of both PEC overexpressing prostate cancer cell lines led to the complete reversal of the EMT phenotype towards a more benign epithelial phenotype (>95% cells) at 18 h.

In vitro, the expression of PEc in prostate cancer cells is induced by the presence of PBMCs. Prostate cancer cells after co-cultured with human PBMCs from 3 different individuals were isolated and analysed by western blot using our anti-PEc MAb for the detection of PEc. Treatment with anti-PEc MAb leads to the detection of more than one band. MS analysis indicated that the Ec peptide copies detected on the blot and on the gel existed as monomers and polymers as well (Fig. S1g) as previously mentioned [5]. Finally, Immunofluorescence analysis (IF) of modified prostate cancer cell lines to overexpress the PEc, further indicated the specificity of this MAb (Fig. S2a).

In vitro effects of anti-PEc MAb in prostate cancer cell lines

Prior to resembling this in-vivo characteristic of prostate tumours, where PEc expression is gradually increased as tumour progresses, in in-vitro models, we genetically modified two prostate cancer cell lines (PC-3 androgen receptor (AR) positive and DU-145 AR negative) to overexpress the PEc without affecting the mIGF-1 levels. Recent evidence suggests that prostate cancer cell lines that overexpress the PEc, present elevated cellular proliferation levels, and a shift of their epithelial phenotype towards a mesenchymal, metastatic phenotype by activating ERK1/2 [7]. Anti-PEc MAb treatment of both prostate cancer cell lines (PC-3PEc and DU145PEc) led to statistically significant decrease of cellular proliferation ($p < 0.0005$ in both cases) as measured at 24 and 48 h (Fig. 1a), in contrast to the unmodified prostate cancer cell lines, where treatment with anti-PEc did not significantly affect cellular proliferation (Fig S2b). Treatment of both modified cell lines with different concentrations of the anti-PEc MAb also leads to a gradual decrease of phosphorylated (activated) ERK 1/2 levels (Fig. 1b). In prostate cancer, ERK1/2 activation apart from cellular proliferation, has been associated with EMT and an increase in metastatic and invasive capacities [15]. MAb treatment resulted in the significant reduction of migration and invasion capacities as was determined by transwell migration and invasion assays ($p < 0.0005$, in both cases) (Fig. 1c). Verification of the anti-PEc MAb effect on the migration (metastatic) ability of the modified prostate cancer cells was obtained by a wound healing assay, where the MAb treated cell lines presented a significantly lower migration rate ($p < 0.0005$ at 18 hours for both cell lines) (Fig. 1d). Examination of the EMT in the MAb treated PEc overexpressing prostate cancer cell lines, suggested the reversal of the PEc associated mesenchymal phenotype, causing the vast majority of the cells to gradually regain their epithelial phenotype (Fig. 1e).

In order to determine if the MAb-enhanced inhibition of cellular proliferation is correlated with the PEc expression levels, we isolated a total of 16 PEc overexpressing clones per cell line and they were separated into four different categories with respect to their PEc expression (Fig S2c). In all the cases MAb treatment of these clones led to almost complete inhibition of the cellular proliferation regardless of the amount of PEc expressed by the cells (Fig. S2d). Prior to investigating the effect of the anti-PEc MAb in the IGF-1R and Insulin Receptor (IR) pathways, the aforementioned MAb was administered in prostate cancer cells followed by the administration of IGF-1 or Insulin, and the pERK 1/2 was examined by western blot. It was determined that the anti-PEc MAb did not affect the IGF-1 nor the IR signalling axis (Fig S2e).

Phosphoproteomics and proteomics analysis of the PEc overexpressing prostate cancer cell lines compared to the wild-type cell lines present significant differences in mainly three pathways (Fig. S6–S10). The MAPK pathway which is also involved in the insulin and IGF-1-induced pathways, is significantly upregulated in the PEc overexpressing cancer cells. The other two pathways that seem to be involved are that of Apoptosis and that of NOD pathway both of which are downregulated in the PEc overexpressing cell lines (Fig. S6a, S7, S8). The phosphoproteomics results were also verified by the proteome analysis of the unmodified prostate cancer cell lines when compared to the PEc

overexpressing prostate cancer cell lines (Fig. S6b, S9, S10). PEc overexpressing cell lines treated with the Anti-PEc MAb presented a protein phosphorylation pattern similar to the wt prostate cancer cell lines (Fig. S6a, S7, S8).

In vivo effects of the anti-PEc MAb in Prostate cancer

The in vivo effects of the anti-PEc MAb were also examined after subcutaneous (sc) inoculation of wild-type (wt) unmodified prostate cancer cell lines (wtPC-3 and wtDU-145) into SCID mice [15]. Both prostate cell lines used can generate tumours in 4 weeks after subcutaneous injection in SCID mice. In this study antibody treatment took place after the determination of palpable tumours in all the cases. Determination of the optimum MAb concentration for prostate cancer treatment was obtained by testing different concentrations of the anti-PEc MAb. The concentrations used were 5, 10, and 20 mg/kg, three times/week. Treatment of prostate tumours with different MAb concentrations resulted in significant tumour growth inhibition in 4 weeks, compared to the tumours treated with the MAb isotype (treatment with isotype control: $1.66 \text{ g} \pm 0.3$, with 0.5 mg/ml anti-PEc MAb $0.62 \text{ g} \pm 0.1$ with 10 mg/ml: $0.18 \text{ g} \pm 0.04$, with 20 mg/ml: $0.16 \text{ g} \pm 0.04$, with Docetaxel: $0.137 \text{ g} \pm 0.05$, $n = 5$, $p < 0.0005$, in every case) (Fig. 2a, b). tumours treated with 10 and 20 mg/kg did not present significant differences with respect to their size and weight, suggesting that the optimum MAb concentration was 10 mg/kg. tumours treated with 10 mg/kg MAb for 4 weeks were also compared with the tumours treated with docetaxel for the same time period, with no significant difference in respect to their size and weight (Fig. 2b).

Immunohistochemical examination of the tumours documented that treatment with the anti-PEc MAb was associated with a significant increase of the epithelial marker E-Cadherin, the reduction of the mesenchymal marker Vimentin, and a decrease of the cellular proliferation marker ki-67 (Fig. 2c). These results were also verified by qRT PCR where the results obtained suggested statistically significant differences in Vimentin, E-Cadherin and Ki-67 expression ($p < 0.0005$ in all the treated vs untreated subjects) (Fig. 2d–f), indicating the efficiency of anti-PEc MAb in ceasing tumour progression. tumours were also examined for the expression of P ERK1/2 (proliferation and EMT). Prostate tumours treated with the anti-PEc MAb presented a significant reduction of P ERK1/2 levels in comparison to the untreated tumours (Fig. 2g).

In a different set of experiments, prostate tumours, resulting from subcutaneous (sc) inoculation of wtPC-3 and wtDU-145 cells into SCID mice, were treated with 10 mg/kg anti-PEc MAb three times/week, for a total of 8 weeks. Tumour volume was measured daily by caliper. Treatment for 5 weeks, led to significant tumour growth inhibition similar to that obtained by docetaxel (10 mg/kg, twice/week) and overall, to a statistically significant size difference when compared with the tumours treated with the isotype control (for PC-3 cells: isotype control: $546 \text{ mm}^3 \pm 57$, anti-PEc MAb: 5 mg/ml: $270 \text{ mm}^3 \pm 45$, 10 mg/ml: $20 \text{ mm}^3 \pm 4$, 20 mg/ml: $18 \text{ mm}^3 \pm 6$, Docetaxel: $18 \text{ mm}^3 \pm 3$, $n = 10$ in every case, $p < 0.005$ similar were the results for DU145 cells), (Fig. 2h, i). The tumour size difference between isotype treated tumours and anti-PEc MAb treated tumours further increased at 60 days (for PC-3 cells: isotype control: $1320 \text{ mm}^3 \pm 212$, anti-PEc MAb: 5 mg/ml: $532 \text{ mm}^3 \pm 105$, 10 mg/ml: $31 \text{ mm}^3 \pm 4$, 20 mg/ml: $26 \text{ mm}^3 \pm 6$, Docetaxel: $28 \text{ mm}^3 \pm 3$, $n = 10$ in every case, $p < 0.0005$ for every case for both cell lines) (Fig. 2h, i).

Effects of the anti-PEc MAb in prostate cancer metastasis. Epithelial to Mesenchymal Transition (EMT) is a central process to metastases, that normally occurs as tumours progress as a response to harsh tumour conditions (space limitation, immune response of the host, hypoxia, NO₂ species). The in vivo observation of the reversal of the cancer mesenchymal phenotype after the administration of the anti PEc MAb, was further

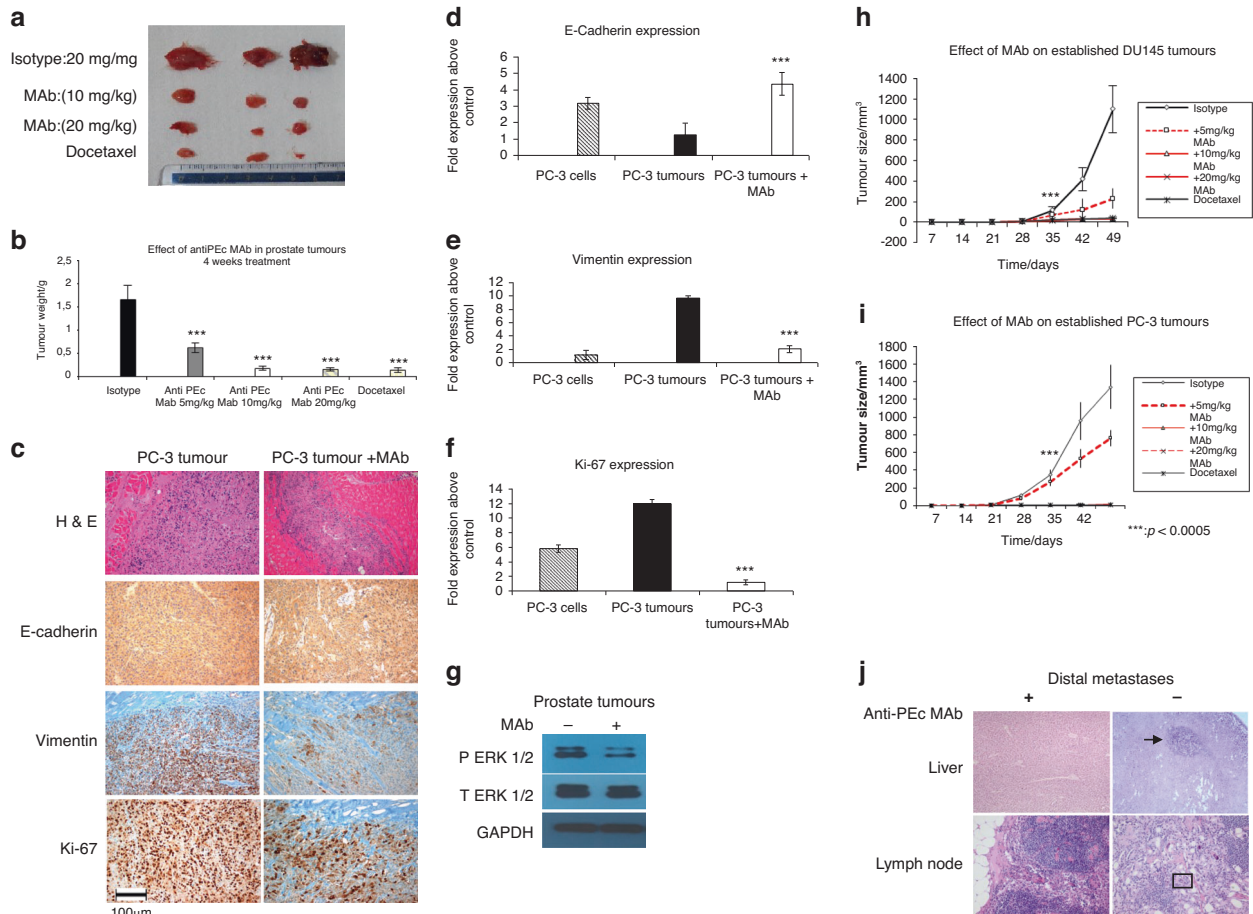


Fig. 2 In vivo analysis of the effects of anti-PEC MAb. **a** wtPC-3 tumours treated with anti-PEC MAb and Docetaxel. Treatment of established tumours with our MAb led to a significant tumour size reduction compared to the untreated tumours. The effects of tumour treatment with 10 mg/kg MAb were similar to the effects of Doc. Treatment (10 mg/kg) at the same duration similar results were obtained in the DU145 tumours. **b** The effects of the anti-PEC MAb were further confirmed by estimating the net weight of the tumours. **c** anti-PEC MAb treated tumours presented evidence of E-cadherin (epithelial marker) upregulation, Vimentin (mesenchymal marker) downregulation, and Ki-67 (proliferation marker) downregulation as determined by IHC. The results obtained by IHC were confirmed by qRT-PCR for E cadherin (**d**), for Vimentin (**e**), and for Ki-67 (**f**). **g** Treatment of tumours with MAb was also associated with the downregulation of P ERK1/2 as was determined by WB analysis. Monitoring the effects of different concentrations of the anti-PEC MAb on prostate cancer tumour size over 50 days, in hormone-sensitive tumours (DU-145) (**h**); and in hormone-resistant tumours PC-3 (**i**). In both cases, treatment with MAb for 35 days was associated with a significant reduction in tumour size. (**j**) 6/10 of the untreated mice presented evidence of sentinel node infiltration (large in-sized weak stained cells with atypic nuclei) with and/or of distal metastases in the liver.

examined in the context of metastasis. Sentinel nodes, as well as different tissues (liver, lungs, kidneys), were collected from SCID mice that developed prostate cancer and they were treated with anti-PEC MAb ($n = 20$). Similarly, the same tissues were collected from untreated controls ($n = 10$). The collection took place 50 days after tumour establishment. In every case, tissues were stained (H&E) and examined by an experienced pathologist till paraffin block exhaustion.

None of the 20 mice treated with the anti-PEC MAb presented evidence of a possible sentinel node infiltration or distal metastases. Six out of the 10 untreated mice presented evidence of sentinel node infiltrations, as was determined by immunohistochemical analysis evaluation and/or by significant size increase. Furthermore, 3 out of the 6 mice presented distal metastases in the liver (Fig. 2j).

Cytotoxic effects of anti-PEC MAb in prostate tumours

Tumour treatment with the anti-PEC MAb apart from the inhibitory effects in respect to tumour size and EMT was also associated with a significant size reduction of the tumours. Further analysis of the tumours by IHC indicated that the tumours treated with the anti-

PEC MAb presented extensive necrosis (H&E stain), which was associated with elevated apoptosis levels as determined by tunnel, caspase 8, and caspase 9 analysis compared to the untreated tumours (Fig. 3a).

Determination of the effect of the anti-PEC MAb in tumour repair process. One of the factors that can induce damage in tumours is the immune system. In vitro and in vivo evidence suggested a significant upregulation of PEC expression in cancer cells and tumours which is associated with the attack of PBMCs and granulocytes [8]. Furthermore, the expression and secretion of the PEC have been associated with the recruitment of stem cells at the same localisation as the granulocytes in SCID mice (to the point of damage). In order to determine the effect of the anti-PEC MAb in the tumour repair by the host stem cells, tumours were generated into SCID mice by subcutaneous introduction of PC-3 or DU-145 cells and MAb treatment took place for 2 weeks (4 doses, 10 mg/kg). Tumours were extracted in the 5th week and 0.3 μ m serial sections were stained for mouse CD45 (IHC) so we could detect the points of attack of granulocytes. Then the immediate next section was stained (IF) with a mouse centromeric probe and anti-

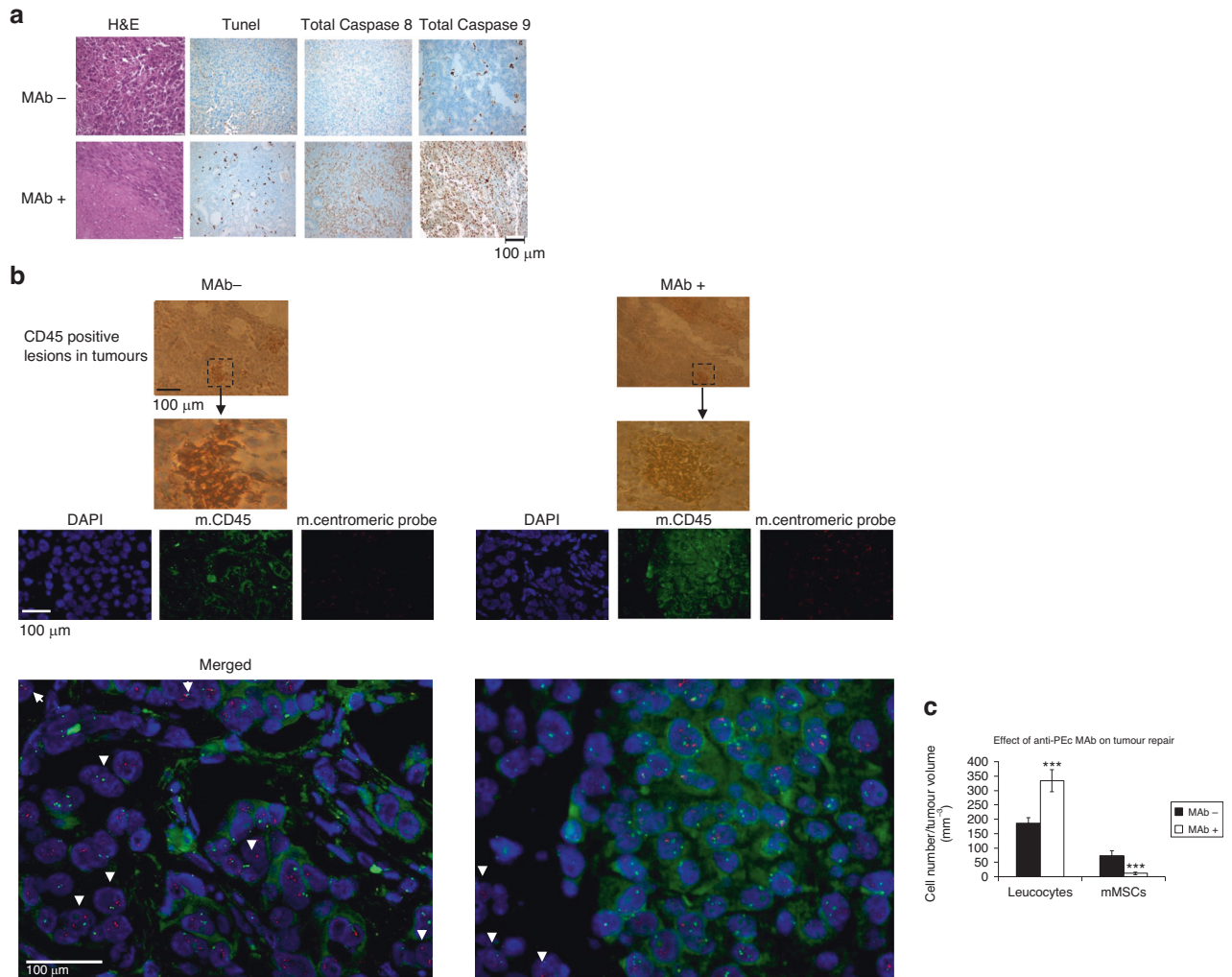


Fig. 3 Effects of anti-PEC MAb on tumour repair and survival. **a** Immunohistochemical analysis of the anti-PEC MAb treated prostate tumours indicated large areas that presented extensive necrosis (H&E stain), which was associated with the induction of apoptosis in the tumours. **b** Mouse CD45 positive lesions on prostate tumours in SCID mice were examined for the presence of CD45 positive mouse cells as detected with a mouse centromeric probe (mouse immune cells) and for CD45 negative mouse cells (mouse mesenchymal stem cells (mmsc)). **c** Treatment with the anti-PEC MAb is associated with a significant decrease of mmsc and a significant increase of mouse immune cells in the tumours.

mouse CD45. CD45 is a marker that is expressed only in leucocytes and since the tumour has been obtained by human cells, tumour cells remained unstained. Mouse leucocytes on the tumour have been stained with CD45 and with the mouse centromeric probe whereas the cells that have only been stained with the mouse centromeric probe are considered to be mouse mesenchymal stem cells (CD45 negative). Our evidence suggests that treatment with the anti-PEC MAb significantly reduced the presence of CD45 negative mouse cells on the tumour ($p < 0.0005$), whereas it significantly increased the number of CD45 positive mouse cells ($p < 0.0005$) (Fig. 3b, c). This is an indication that anti-PEC MAb treatment results in the enhanced immune reaction of the host organism towards the tumour.

Anti-PEC MAb tumour toxicity is associated with antibody-dependent cellular cytotoxicity. Prior to explaining the *in vivo* cancer cytotoxicity associated to the anti-PEC MAb, three models were generated to resemble the *in vivo* mechanism of the immune cytotoxic effect towards the tumour. The effect of the complement-dependent cytotoxicity of the anti-PEC MAb on prostate tumours was examined by incubating prostate cancer cells with the serum from five different individuals. Cellular

viability was measured at 24 and 48 hours after MAb administration. The serum antibody-dependent cellular cytotoxicity of the anti-PEC MAb was examined by the incubation of prostate cancer cells with peripheral blood mononuclear cells (PBMCs) from the same individuals followed by the administration of the anti-PEC MAb. Cellular viability was then measured at 24 and 48 h. Finally, the effects of the complement-dependent cellular cytotoxicity on the anti-PEC MAb treated cells were examined by incubating the prostate cancer cells with the serum and PBMCs of the above healthy individuals followed by the administration of the anti-PEC MAb. Each co-incubation was allowed a 24-hour incubation; in order for the prostate cancer cells to express the PEC. Then the anti-PEC MAb administration followed. After 24 and 48 h the cancer cells were isolated from the PBMCs with CD45 coated magnetic beads and they were analysed by trypan blue and MTT analysis. Our evidence indicates that the effects of the anti-PEC MAb in prostate tumours in respect to survival are generated by the serum antibody cellular cytotoxicity. Treatment with anti-PEC MAb of prostate cancer cells co-incubated with PBMCs resulted in a significant decrease of prostate cancer cells at 24 and 48 h compared to the untreated co-cultures ($p < 0.005$ and $p < 0.0005$, respectively) (Fig. 4a).

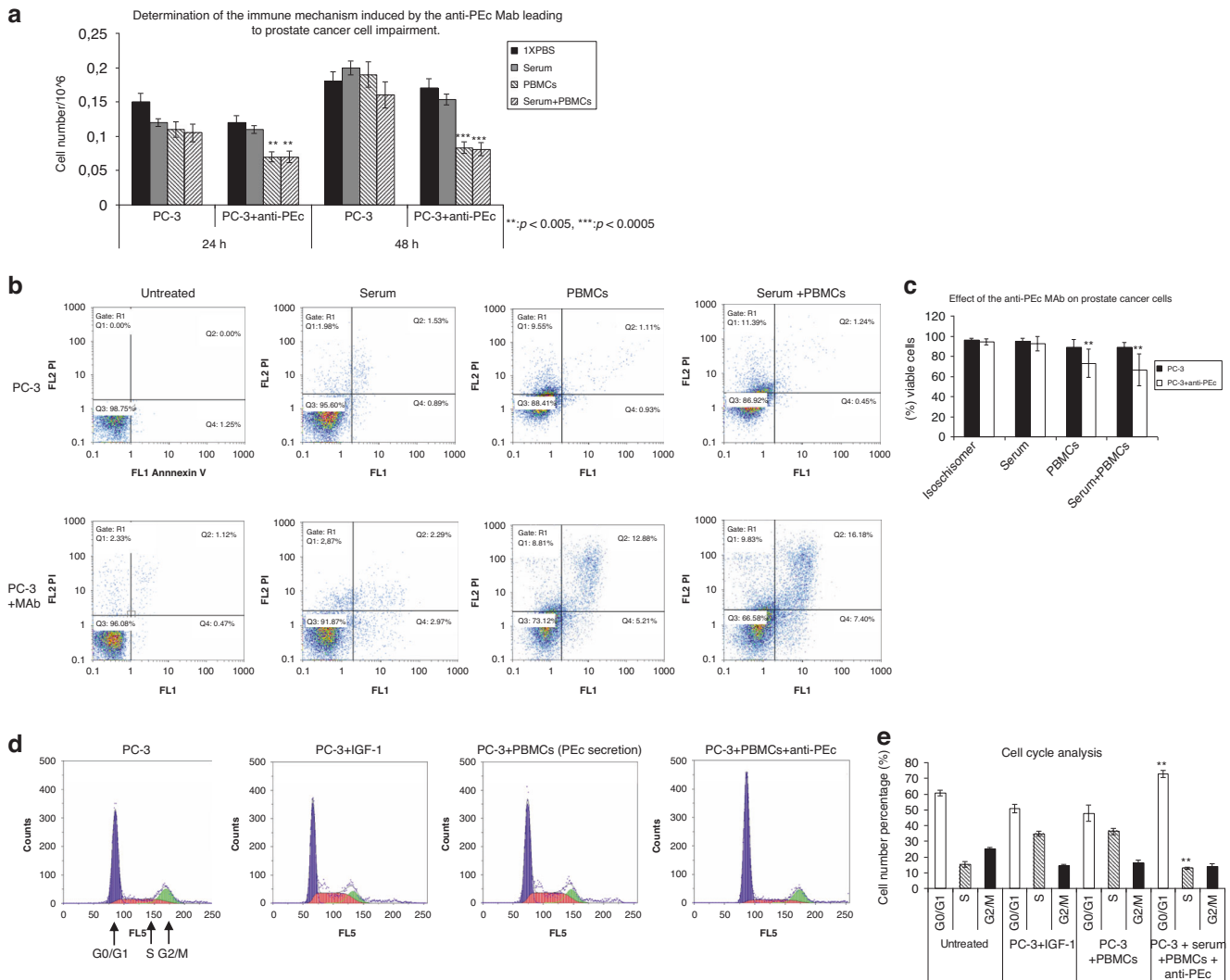


Fig. 4 Determination of the immune mechanism involved in anti-PEC-induced tumour cytotoxicity. **a** Analysis of the complement-dependent cytotoxicity, the serum antibody-dependent cellular cytotoxicity, and of the complement-dependent cellular cytotoxicity that may be induced by the anti-PEC MAb on prostate tumours was examined with respect to cellular viability at 24 and 48 hours after MAB administration. The anti-PEC MAB significantly impairs the cellular proliferation of prostate cancer cells in the presence of PBMCs. **b, c** Flow cytometry with Annexin/PI indicated that treatment of prostate cancer cells with anti-PEC MAB significantly induced apoptosis in prostate cancer cells, PBMCs co-cultures. **d, e** Cell cycle analysis of prostate cancer cells expressing PEC indicates that treatment with anti-PEC MAB leads to G0/G1 arrest and to a significant reduction of the cells entering the S phase.

Analysis of the effects of the immune system in prostate cancer cells after anti-PEC MAB treatment. The cancer cell impairment after anti-PEC treatment, in the presence of the PBMCs was further examined aiming to determine if these cells are involved in the tumour anti-PEC MAB induced apoptosis/necrosis observed in our *in vivo* models. For that purpose, prostate cancer cells were allowed to interact with either serum (complement-dependent cytotoxicity), PBMCs (antibody-dependent cellular cytotoxicity), or serum and PBMCs (complement-dependent cellular cytotoxicity) from 5 healthy individuals, for 24 hours and they were then incubated with the anti-PEC MAB for another 12 hours. The cancer cells were isolated from PBMCs with CD45 magnetic coated beads (materials and methods) and analysed with Annexin and propidium iodide for apoptosis and with DAPI for their cell cycle. Cancer cells treated with the anti-PEC MAB in the presence of PBMCs presented a significant increase in the levels of apoptosis and necrosis when compared to untreated cancer cells or to MAB-treated cells but without PBMCs (Fig. 4b, c). Additionally, MAB-treated cancer cells that have been exposed

to PBMCs presented a significantly higher number of cells at G0/G1 phase and a significantly lower number of cells at S phase of the cell cycle compared with the untreated cells (Fig. 4d, e, $p < 0.005$ in both cases). The fact that the co-incubation of MAB-treated cancer cells with PBMCs and with PBMCs with serum is not associated with a significant difference in respect to apoptosis, cell cycle, or survival, indicates that the MAB exerts its cytotoxic actions through antibody-dependent cellular cytotoxicity.

Introduction of PEC Knock Down (KD) PC-3 and DU-145 cells. In order to determine the *in vivo* effect of the complete absence of the PEC peptide, SCID mice were also subcutaneously introduced to prostate cancer cells that silenced the PEC expression without affecting the expression of mature IGF-1. None of these mice ($n = 10$) developed palpable tumours 10 weeks after cancer cell inoculation. The controls that were injected with wt prostate cancer cells developed palpable tumours at 25–30 days, $n = 10$.

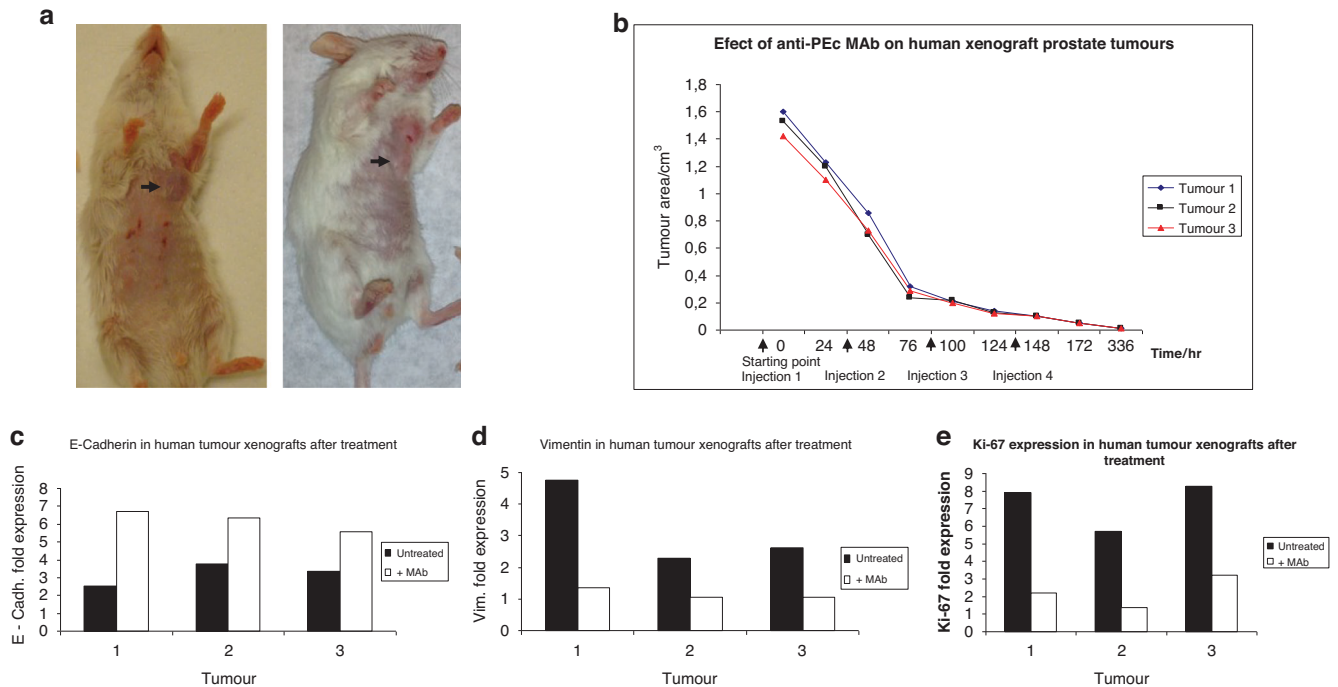


Fig. 5 Effects of anti-PEc MAb treatment on human prostate cancer xenografts. **a, b** Xenografts from three human prostate tumours were injected into SCID mice and allowed to reach 1.5 cm³. Intravenous administration of 10 mg/kg anti-PEc every 48 h (4 injections) led to a significant tumour size reduction starting from the second injection. **c** E-cadherin qRT-PCR analysis presented a significant upregulation in all the tumours examined. **d** Vimentin presented evidence of at least 50% downregulation in all the tumours examined. **e** Ki-67 presented evidence of at least a 70% reduction in all the tumours treated. The 'untreated' levels of expression of E-Cadherin, Vimentin, and Ki-67 were estimated by the initial raw material provided to us. Statistical analysis was not performed due to the small sample (3 tumours) and due to the fact that each tumour presented different initial characteristics with respect to E-Cadherin, vimentin, and Ki-67 expression.

PEc expression in prostate cancer patient biopsies

The levels of expression of IGF-1Ec were also examined in 100 early-stage (non-metastatic) prostate cancer patients (Fig. S3a). Immunohistochemical expression of stained proteins was classified as either grade 1 (weak intensity), grade 2 (moderate intensity), or grade 3 (strong intensity). The H scoring system, incorporating both intensity and distribution of staining, was used for semi-quantitative analysis of protein immunoreactivity. More specifically, the percentage of positive cells was measured in every section and multiplied by 1, 2, and 3, respectively (grade 1 score = percentage with grade 1 expression × 1; grade 2 score = percentage with grade 2 expression × 2; grade 3 score = percentage grade 3 expression × 3). A total score between 0 and 300 was obtained for each case (total score = grade 1 score + grade 2 score + grade 3 score) (Fig. S3a). In all the cases elevated IGF-1Ec was associated with, the upregulation of vimentin and Ki-67 and the downregulation of E cadherin and PTEN protein (Fig. S3a).

The IGF-1Ec h score was found significantly lower in prostate tumours in patients of stage T2N0 (AJCC) as compared to the tumours of patients of stage T3aN0 ($p < 0.0005$). Patients of stage T3aN1 and T3bN0, presented significantly higher tumour IGF-1Ec levels compared to that of T3N0 patients ($p < 0.0005$) (Fig. S3b, c). All of our patients were of Gleason Score 6, 7, and 9. IGF-1Ec expression was significantly higher in the patients with Gleason score 7 compared to those with Gleason score 6 ($p < 0.005$). Patients with a Gleason score of 9 presented significantly higher levels of IGF-1Ec compared to those with a Gleason score 7 ($p < 0.0005$) (Fig. S3d). Similarly, patients who presented extraprostatic extension were significantly associated with elevated PEc expression ($p < 0.0005$) (Fig. S3e).

Tumour cribriform architecture seems to be another factor that is associated with the IGF-1Ec expression levels. Higher cribriform

grade was associated with significantly elevated levels of IGF-1Ec compared to tumours with lower cribriform ($p < 0.0005$) (Fig. S3f). Finally, elevated seminal vesicle infiltration presented significantly higher IGF-1Ec levels than prostate tumours that were not associated with invasive potential ($p < 0.0005$ in both cases) (Fig. S3g).

Effect of the anti-PEc MAb on human prostate tumour xenografts

Approximately 0.7 cm³ of prostate tumours from 3 individuals with prostate cancer (all of which were of stage T3bN1M0 and high Gleason score 8–9) were donated to us after total prostatectomies and tumour characterisation. Informed consent was obtained in every case.

Human xenografts from prostate cancers were generated after sc inoculation of about 0.5 cm³ of tumour into SCID mice ($n = 3$). The lump disappeared in 3 days and palpable tumours developed in 13 to 19 weeks (tumour 1 in 13 weeks, tumour 2 in 18 weeks, tumour 3 in 19 weeks). Tumours were allowed to grow up to 1.5 cm³ and they were then treated with 20 mg/ml anti-PEc MAb intravenously for a period of 14 days during which mice were subjected to 4 injections. Starting point at time 0 was set as the point where tumour area was about 1.5 cm³, the second injection was obtained at 48 h, the 3rd at 100 h, and the 4th at 148 h. Treatment of SCID mice with anti-PEc MAb resulted in a significant reduction in tumour area in 76 hours (from 1.5 cm³ ± 0.1 to 0.3 ± 0.02, $p = 0.0003$) (Fig. 5a). Tumour area decreases continued over the whole period of monitoring but with a lower rate (Fig. 5b). At day 14 (336 h) tumours were extracted and measured. The tumour area in all the cases was about 0.1 cm³ as measured by caliper.

Analysis and comparison of the epithelial marker E-cadherin, the mesenchymal marker Vimentin and the proliferation marker

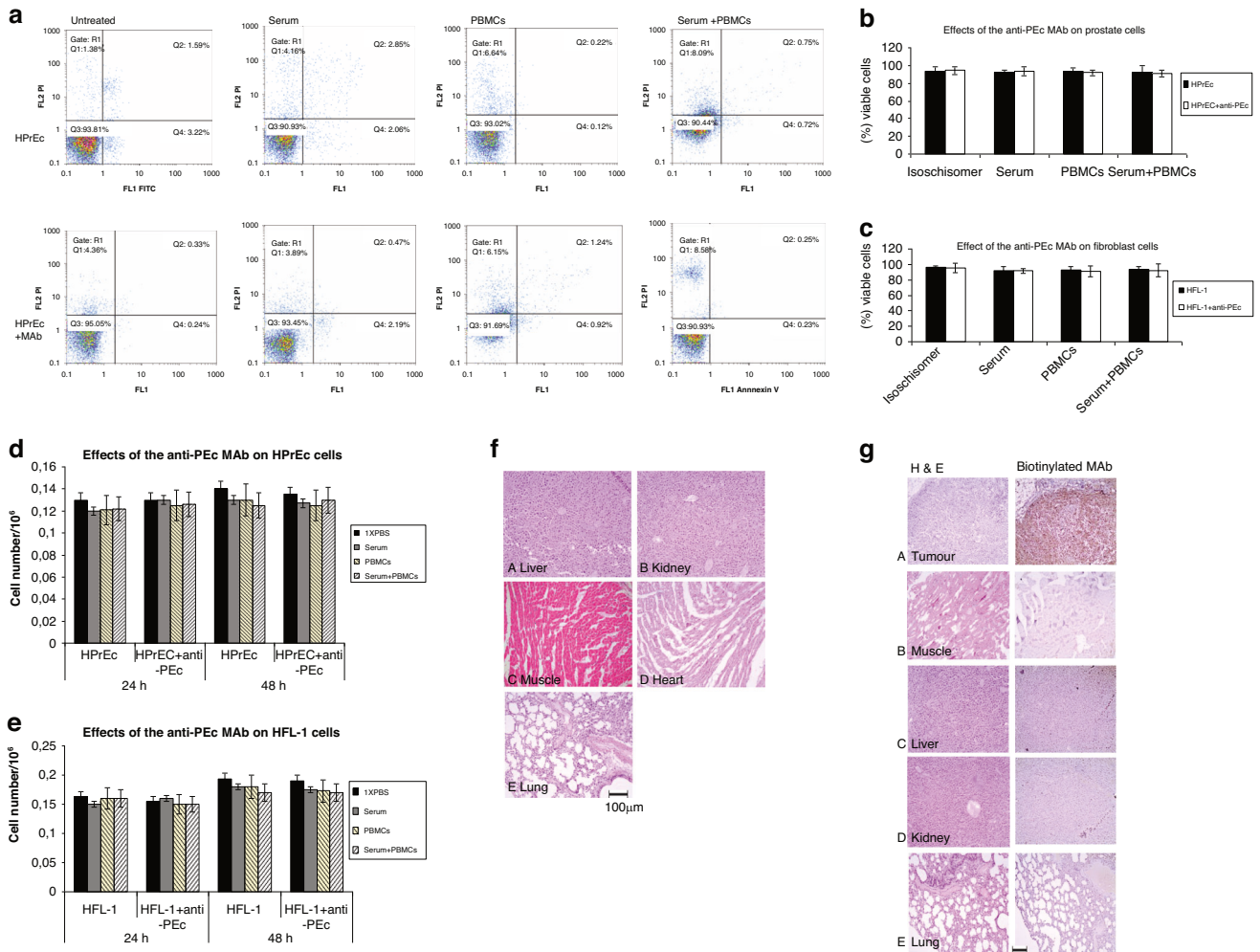


Fig. 6 Anti-PEC MAb off-target effects and specificity. a–c Flow cytometry Annexin/PI analysis. Examination of the effects of anti-PEC MAb on the induction of apoptosis in the presence of serum, PBMCs, and serum and PBMCs. No statistically significant difference was observed when each case was compared with the corresponding control. d Cell viability analysis of normal prostate cells (d) and of normal fibroblast cells (e) treated with the anti-PEC MAB in the presence of serum, PBMCs, and serum plus PBMCs at 24 and 48 hours did not present evidence of toxicity of the anti-PEC MAB used. f Treatment of wt mice with 30 mg/kg anti-PEC MAB 4 times/week for 60 days was not associated with any tissue structural alterations or deterioration. g MAB tissue distribution analysis suggests that the anti-PEC MAB used is not detected in any of the tissues examined apart from the tumour.

Ki67 of the human tumours before inoculation into SCID mice and after treatment with anti-PEC MAB indicated a significant reduction in the levels of Vimentin ($p < 0.0005$ combined cases), a significant increase of E-Cadherin levels ($p < 0.0005$ combined cases) and a significant decrease of Ki67 levels ($p < 0.0005$ combined cases) (Fig. 5c–e). The results obtained indicate a reduction in cellular proliferation and a switch of the cancer mesenchymal cells which are associated with metastases and invasion, towards a more “benign” epithelial phenotype. Sentinel nodes as well as livers and lungs were examined for metastases (IHC). None of these tissues exhibited evidence of infiltration.

Anti-PEC MAb toxicity and tissue distribution

In vitro: The *in vitro* off-target effects of the anti-PEC MAB were examined in two normal human cell lines, one prostate (HPrEc) and one fibroblast (HFL-1). In this case, the normal cells were incubated with either, serum, PBMCs, or serum and PBMCs from 5 different individuals. After 24 hours the anti-PEC MAB was introduced for 12 hours and the non-cancerous cells were isolated from the PBMCs and analysed with Annexin/PI, prior to determining the levels of apoptosis-associated with the anti-PEC MAB. No significant differences were observed with respect to the

induction of apoptosis after the administration of anti-PEC MAB in both normal cell lines used, nor when the administration of the anti-PEC MAB was obtained in the presence of serum, PBMCs, and serum +PBMCs (Fig. 6a–c).

In vitro to determine the effects of the anti-PEC MAB in normal cell survival over 48 hours, non-cancerous cells were introduced with either, serum, PBMCs, or serum and PBMCs from 5 healthy individuals for 24 hours followed by the introduction of the anti-PEC MAB. The non-cancerous prostate and fibroblast cells were isolated after 24 and 48 h and counted by trypan blue and MTT analysis. No statistically significant differences were observed in any of the comparisons between MAB-treated and untreated cell lines (Fig. 6d, e), indicating that in *in vitro* conditions, the anti-PEC MAB is not associated with any cytotoxic effects and this is evident due to the fact that non-cancerous cells produce almost negligible amounts of PEC even when challenged with factors of the immune system.

In vivo: The anti-PEC MAB was examined for toxic side effects as well as for its distribution in mouse tissues. For the toxicity determination, 10 wt mice ($n = 10$) were injected 4 times/week with 30 mg/kg anti-PEC MAB for 60 days. Mice were assessed daily

with respect to their appearance (body weight and coat condition), body function (dyspnoea and/or tachypnoea, food intake), environment (loose stools or diarrhoea, blood in diarrhoea), and behaviour (handling, aggression, abnormal gait, abnormal posture, reluctance to move), according to the Severity Assessment Framework of the European Commission.

None of the characteristics examined presented significant differences between treated and untreated mice. At the end of 60 days, mice were sacrificed and tissues were collected stained, and analysed with respect to tissue and cellular integrity. The tissues examined were lungs, liver, kidneys, heart, and muscle. None of the tissues examined presented evidence of deterioration or structural alterations as assessed by an experienced pathologist (Fig. 6f).

Tissue distribution

The tissue distribution of the MAb examined in this study was carried out using the biotinylated version of the anti-PEc MAb. Five SCID mice ($n = 5$) with already established tumours were injected with 20 mg/kg biotinylated MAb. After 24 h, mice were sacrificed and tissues were collected and analysed with an anti-biotin MAb. Tissues and tumours were then collected and examined for the presence of the anti-PEc MAb with an anti-biotin antibody (Abcam). The tissues examined were lung, liver, muscle, and kidney. It was determined that anti-PEc MAb was only present in the tumour and it was undetectable in all the healthy tissues examined (Fig. 6g).

Alternative means of targeting the pathway

The IGF axis plays important roles in cancer progression and metastasis [15]. The PEc arises from the proteolytic cleavage of the IGF-1Ec isoform. Recent evidence suggests that the PEc exerts its actions similarly to the IGF-1 through ERK1/2. anti-IGF-1R MAb and anti-IGF-1MABs are in clinical trials for a number of different solid neoplasms. We therefore compared the effects of anti-IGF-1R and anti-IGF-1 MABs to those exerted by the anti-PEc MAb in prostate tumours. Subcutaneous prostate tumours were obtained by the introduction of PC-3 or DU145 cells in SCID mice. Tumours were treated for 4 weeks with 10 mg/kg of anti-IGF-1 MAB [15], anti-IGF-1R MAB [15] and anti-PEc MAB. All the tumours extracted presented a significant size reduction compared to the tumours treated with the isotype control (Isotype treatment: $1.73 \text{ g} \pm 0.19$, anti-IGF-1R: $1.148 \text{ g} \pm 0.082$, anti-IGF-1: $1.07 \text{ g} \pm 0.082$, anti-PEc MAB: $0.062 \text{ g} \pm 0.012$, $n = 10$ in every case, $p < 0.005$) (Fig. S4a–c). They also presented a significant increase in E cadherin expression ($p < 0.005$) (Fig. S4d) and a decrease in Vimentin and Ki-67 expression ($p < 0.005$ in both cases) as determined by qRT-PCR (Fig. S4e, f). Comparison of the tumours treated with the anti-IGF-1 and anti-IGF-1R antibody (both from R&D Systems, Inc., MN, USA) did not present significant difference in the aforementioned markers. Comparison of the tumours treated either with the anti-IGF-1 Ab or the anti-IGF-1R antibody with the anti-PEc MAB indicated a significant difference in tumour size (Fig. S4a–c) and in the expression of E cadherin and vimentin ($p < 0.0005$ in every case, Fig. S4d–f). Sentinel nodes as well as livers and lungs were examined for metastases (IHC). None of these tissues exhibited evidence of infiltration. Toxicity: IGF-1R and IGF-1 MAB treated mice appeared to be lethargic and in 2 and 3 out of 10 respectively presented diarrhoea.

The effect of anti-PEc MAB in breast and colon cancer

The effect of the anti-PEc MAB was also examined in SCID mice that developed breast cancer after orthotopic inoculation of MCF-7 cells ($n = 20$) and colon cancer after subcutaneous injection of DLD-1 cells ($n = 10$), with similar results. In both cases, the protocol for the antibody administration was kept the same as in prostate cancer. Therefore, after tumour establishment, 10 mg/kg were administered into the SCID mice.

In breast cancer 2 out of 20 mice treated with the anti-PEc MAB retained palpable tumours compared to 10 out of 10 obtained in the untreated mice, 4 weeks after tumour detection (Fig. S5a). Due to the small size of the tumours obtained by the MAB-treated mice, we were not able to proceed with IHC (Fig. S5b). Therefore, we proceeded with qRT-PCR to examine the levels of E-Cadherin, Vimentin, and Ki-67. Similarly, to the results observed in prostate cancer, breast tumours presented evidence of EMT reversal associated with a significant decrease of Vimentin and Ki-67 ($p < 0.0005$ for both markers) and an increase of E-Cadherin compared to the untreated tumours ($p < 0.0001$) (Fig. S5c).

SCID mice with sc colon cancer tumours have been developed using wt DLD-1 cells. Due to the fact that the colon cancer cells used, presented much higher proliferation rate and invasive capacity than those used in prostate and breast cancer, we used the highest antibody concentration tested in the experiment for the determination of the optimum anti-PEc MAB concentration. Treatment of palpable tumours with the anti-PEc MAB (4 weeks, 3 times/ week, 20 mg/kg) resulted in the development of significantly smaller tumours compared to the untreated tumours (Isotype treatment: $2.36 \text{ g} \pm 0.29$, anti-PEc MAB treatment: $1.23 \text{ g} \pm 0.16$, Docetaxel treatment: $0.38 \text{ g} \pm 0.06$, $n = 10$, $p < 0.0005$) (Fig. S5d). Treated tumours presented significantly lower levels of Vimentin and Ki-67 expression and elevated levels of E cadherin as was observed by IHC and qRT-PCR ($p < 0.0005$ in every case) (Fig. S5e). Western blot analysis also presented evidence of pERK 1/2 reduction compared to the untreated tumours (Fig. S5f). Tumours that are given rise by DLD-1 cells are very aggressive and they have high infiltrating capacity [16]. What was observed in respect to tumour infiltration is the fact that DLD-1 tumours treated with the anti-PEc MAB did not infiltrate into the mouse body, compared to the untreated tumours where in all cases tumours infiltrated the ribcage and other tissues (Fig. S5g).

DISCUSSION

The current treatment options for cancer have shifted more towards targeted therapies rather than traditional chemotherapy. Immunotherapy, using engineered antibodies or antibody fragments, directly targeting tumour cells or inducing anti-tumour immune responses, is now considered a main component of cancer therapy.

The IGF system is gaining tremendous interest and has become one of the most explored areas in targeted anticancer therapy over the last decade since it is involved in several aspects of cancer development such as tumour growth, metastasis, and invasion in a broad range of malignancies. Current therapeutic targeting of the IGF-1 signalling pathways focuses on blocking the IGF-1R or targeting the IGF-1R major ligand (IGF-1) [15–20]. Targeting of the IGF-1 system apart from the obvious toxicity defects associated to its natural function [21–24] of the targeting of the IGF-1 system, seems to be problematic since none of these therapies was associated with significantly better overall survival in patients treated with chemotherapy and anti-IGF-1R or anti-IGF-1 vs patients treated with chemotherapy in various cancers. In the case of monoclonal antibodies against IGF-1R, it has been suggested that they can act as “biased” IGF-1R agonist to promote IGF-1R/b-arrestin1 association. This association results in ERK1/2 signalling pathway activation. Furthermore, these antibodies cannot neutralise the nuclear pool of the IGF-1R that possesses pro-tumorigenic activities. In the case of monoclonal antibodies against IGF-1 there are several Phase II and Phase III clinical trials with encouraging results.

Unlike IGF-1, the IGF-1Ec isoform is not normally expressed in healthy tissues. Its expression seems to be associated with tissue damage where its main function is HMSC mobilisation prior to repair [25–27]. In cancer, IGF-1Ec is only produced when prostate tumours (or cancer cells) are challenged. In this case, there is the

production of the IGF-1Ea isoform (the main mature IGF-1 producing isoform) and the production of the IGF-1Ec isoform that increases as tumour progresses. The IGF-1Ec isoform is cleaved and it yields the mature IGF-1 and the PEc. Both molecules (IGF-1 and PEc) exert oncogenic actions through different receptors. Targeting of the IGF-1 or the IGF-1R covers a broad range of molecules involved in the IGF-1 system, including the IGF-1R and the heterohybrid receptors but it does not affect the action of PEc, similar is the case with the anti-IGF-1 MABs. Therefore, in any treatment applied, it seems that the PEc is not affected in any case. The dramatic increase of PEc levels as tumour progresses compared to IGF-1 levels indicates the importance of PEc in tumour progression.

Histopathology studies in cancer patients, using an in-house anti-PEc polyclonal antibody, suggest that the presence of PEc is evident in various solid tumours including prostate, breast, endometrial, thyroid, and colon cancer where is significantly associated with advanced stages [28–32].

Having that in mind a monoclonal anti-PEc antibody was developed and it was initially tested vs the polyclonal anti-IGF-1Ec, previously developed, for its specificity for PEc in human prostate tumours. Both antibodies presented similar specificity with respect to PEc detection in human tumours. PEc expression was significantly associated to Gleason score, stage, and lymph node infiltration. In vitro, testing of the anti-cancer effects of the anti-PEc MAB took place using prostate cancer cell lines. The majority of cancer cell lines express a very small amount of PEc when unchallenged, in in vitro conditions. For that reason, we used prostate cancer cell lines modified to overexpress the PEc peptide, prior to mimic the in vivo “natural” tumour growth. In this case, anti-PEc administration was associated with a significant decrease in cellular proliferation and reversal of the cancer mesenchymal phenotype towards a more benign, epithelial phenotype, which explains the decrease in migration and invasion abilities of those cells. In vivo testing of the anti-PEc MAB in prostate cancer models lead to a significant decrease in proliferation and metastatic rate which was associated with a decrease of the Ki-67 expression (proliferation marker), of the mesenchymal marker Vimentin and an increase of the epithelial marker E-Cadherin. Treatment of prostate tumours developed in SCID mice, with anti-PEc MAB over a 7-week period of time, indicated significant tumour size reduction similar to that obtained by docetaxel.

The anti-PEc MAB was also tested in human prostate xenograft tumours. In this case, tumours were allowed to reach 1.5 cm³ in volume before anti-PEc MAB administration. Treatment was associated with a significant decrease in the tumour volume in every case and a reversal of the mesenchymal phenotype.

Our evidence indicates that the anti-PEc MAB inhibits tumour growth and metastasis but the mechanism explaining its' contribution to the decrease in tumour size is not yet clear. IHC analysis of the anti-PEc treated tumours indicated the presence of large necrotic regions that were associated with significantly elevated apoptotic rate. PEc is involved in tumour repair by inducing the mobility of host stem cells towards the tumor. Treatment of prostate tumours with anti-PEc significantly suppressed the tumour ability to attract MSC affecting the balance between immune damage and repair in the tumor. tumour damage is associated with the exposure of more immunogenic tumour antigens and the mobilisation of more leucocytes towards the tumour site. The fact that the level of host leucocytes in the tumour was significantly higher, supports this hypothesis and may be the answer to the anti-PEc MAB effect on tumour size. Furthermore, evidence obtained by the in vitro analysis indicated that the anti-PEc MAB is associated with tumour cell cycle arrest in G0/G1 phase and its tumour toxicity is associated with antibody-dependent cellular cytotoxicity leading to a significant increase in apoptosis and necrosis.

The role of PEc in cancer development was further examined by a series of PEc KD experiments. The fact that the PEc KD cell lines failed, in their vast majority, to lead to the development of solid tumours is an indication of the necessity of the PEc peptide in tumour establishment and progression.

Analysis of the off-target effects was obtained both in non-cancerous cell lines and in mice. Prior to allowing the cells to produce small levels of PEc they were co-cultured with PBMCs. Treatment of these cells with the anti-PEc MAB did not affect the cellular proliferation rate, or cell cycle nor was associated with a significant elevation of apoptotic/necrotic cells. Our in vivo evidence indicated that the mice participating in this study were not affected with respect to their tissue integrity (IHC), appearance, behaviour, environment, and body function, even when exposed to high doses of MAB for a prolonged period of time. Whereas the present anti-PEc MAB seems to be highly specific for the PEc as it was only observed in the tumour and it is undetectable in all the normal tissues examined.

The effects of the anti-PEc MAB were also compared with the effects of two antibodies targeting the IGF axis, the anti-IGF-1 and the anti-IGF-1R. Both anti-IGF-1 and anti-IGF-1R antibodies were associated with significant inhibition of tumour growth and reversal of EMT. Anti-PEc MAB treated tumours presented, a significant decrease in size, and EMT reversal (significant decrease of Vimentin and Ki67 levels and a significant increase of E-Cadherin). Both factors IGF-1 and PEc seem to share a common pathway that is associated to cellular proliferation and EMT and both are increasing as tumour progresses. The fact that both factors have similar actions on cancer cells with the exception of the effects of PEc on mesenchymal cells mobilisation, may be an indication of a synergistic action between these two factors through two different receptors! The fact that the anti-PEc MAB treatment yields significantly better tumour outcome, may be associated with the anti-PEc capacity to inhibit stem cell mobilisation leading to the inhibition of tumour repair and to the exposure of the tumour antigens to the host immune system thus indirectly, inducing the attack of the immune system towards the tumor.

The anti-PEc MAB was also tested in breast and colon cancer in vivo models in a pilot study with similar results in both cases as in prostate cancer. These pilot results present a strong indication of the potential usefulness of this MAB in other cancers too.

This study investigated the potential efficacy of our monoclonal Anti-PEc MAB as a targeting agent directly aiming at the mechanisms through which PEc promotes cancer development and advancement. The evidence procured regarding both the anti-cancer development potential and the lack of toxicity encourages us to further investigate the role of the anti-PEc MAB as a prospective therapeutic agent against human cancer.

DATA AVAILABILITY

1. The proteomics and phosphoproteomics datasets generated during and/or analysed during the current study have been deposited (and are available) to the ProteomeXchange Consortium via the PRIDE (Perez-Riverol et al., 2019) partner repository with the dataset identifier (title of the paper or the name of the corresponding author). 2. All the rest of the data generated or analysed during this study are included in this published article [and its supplementary information files].

REFERENCES

1. Liu G, Zhu M, Zhang M, Pan F. Emerging role of IGF-1 in prostate cancer: a promising biomarker and therapeutic target. *Cancers*. 2023;15:1287.
2. Brahmkhatri VP, Prasanna C, Atreya HS. Insulin-like growth factor system in cancer: novel targeted therapies. *Biomed Res Int*. 2015;2015:538019.
3. Pierce JR, Martin BJ, Rarick KR, Alemany JA, Staab JS, Kraemer WJ, et al. Growth hormone and insulin-like growth Factor-I molecular weight isoform responses to resistance exercise are sex-dependent. *Front Endocrinol (Lausanne)*. 2020;21:571.

4. Ascenzi F, Barberi L, Dobrowolny G, Villa Nova Bacurau A, Nicoletti C, Rizzuto E, et al. Effects of IGF-1 isoforms on muscle growth and sarcopenia. *Aging Cell*. 2019;18:e12954.
5. Dai Z, Wu F, Yeung EW, Li Y. IGF-1Ec expression, regulation and biological function in different tissues. *Growth Horm IGF Res*. 2010;20:275–81.
6. Matheny RW Jr., Nindl BC, Adamo ML. Minireview: Mechano-growth factor: a putative product of IGF-1 gene expression involved in tissue repair and regeneration. *Endocrinology*. 2010;151:865–75.
7. Schlegel W, Raimann A, Halbauer D, Scharmer D, Sagmeister S, Wessner B, et al. Insulin-like growth factor I (IGF-1) Ec/Mechano Growth factor-a splice variant of IGF-1 within the growth plate. *PLoS One*. 2013;8:e76133.
8. Armakolas A, Philippou A, Panteleakou Z, Nezos A, Sourla A, Petraki C, et al. Preferential expression of IGF-1Ec (MGF) transcript in cancerous tissues of human prostate: evidence for a novel and autonomous growth factor activity of MGF E peptide in human prostate cancer cells. *Prostate*. 2010;70:1233–42.
9. Armakolas A, Kaparelou M, Dimakakos A, Papageorgiou E, Armakolas N, Antonopoulos A, et al. Oncogenic role of the Ec peptide of the IGF-1Ec isoform in prostate cancer. *Mol Med*. 2015;21:167–79.
10. Armakolas A, Dimakakos A, Loukogiannaki C, Armakolas N, Antonopoulos A, Florou C, et al. IL-6 is associated to IGF-1Ec upregulation and Ec peptide secretion, from prostate tumours. *Mol Med*. 2018;24:6.
11. Savvani A, Petraki C, Msaouel P, Diamanti E, Xoxakos I, Koutsilieris M. IGF-1Ec expression is associated with advanced clinical and pathological stage of prostate cancer. *Anticancer Res*. 2013;33:2441–5.
12. Xoxakos I, Petraki C, Msaouel P, Armakolas A, Grigorakis A, Stefanakis S, et al. Expression of Kisspeptin (KISS1) and its Receptor GPR54 (KISS1R) in prostate cancer. *Anticancer Res*. 2020;40:709–18.
13. Bastide C, Bagnis C, Mannoni P, Hassoun J, Bladou F. A Nod Scid mouse model to study human prostate cancer. *Prostate Cancer Prostatic Dis*. 2002;5:311–5.
14. Tanaka S, Kobayashi W, Haraguchi M, Ishihata K, Nakamura N, Ozawa M. Snail1 expression in human colon cancer DLD-1 cells confers invasive properties without N-cadherin expression. *Biochem Biophys Res*. 2016;8:120–6.
15. Li H, Bath IS, Qu X, Xu L, Song N, Wang R, et al. IGF-1R signaling in epithelial to mesenchymal transition and targeting IGF-1R therapy: overview and new insights. *Mol Cancer*. 2017;16:6.
16. Osher E, Macaulay VM. Therapeutic targeting of the IGF axis. *Cells*. 2019;8:895.
17. Simpson A, Petnga W, Macaulay VM, Weyer-Czernilofsky U, Bogenrieder T. Insulin-Like Growth Factor (IGF) pathway targeting in cancer: role of the IGF axis and opportunities for future combination studies. *Target Oncol*. 2017;12:571–97.
18. Gao J, Chesebrough JW, Cartlidge SA, Ricketts SA, Incognito L, Veldman-Jones M, et al. Dual IGF-1/II-neutralizing antibody MEDI-573 potently inhibits IGF signaling and tumour growth. *Cancer Res*. 2011;71:1029–40.
19. Olmos D, Okuno S, Schuetz SM, Paccagnella ML, Yin D, Gualberto A, et al. Safety, pharmacokinetics and preliminary activity of the anti-IGF-1R antibody CP-751,871 in patients with sarcoma. *JCO Suppl*. 2008;6:122.
20. Kurzrock R, Patnaik A, Aisner J, Warren T, Leong S, Benjamin R, et al. A phase I study of weekly R1507, a human monoclonal antibody insulin-like growth factor-1 receptor antagonist, in patients with advanced solid tumours. *Clin Cancer Res*. 2010;16:2458–65.
21. Al-Sameria S, Radovick S. The role of Insulin-like Growth Factor-1 (IGF-1) in the control of neuroendocrine regulation of growth. *Cells*. 2021;10:2664.
22. Yakar S, Rosen CJ, Beamer WG, Ackert-Bicknell CL, Wu Y, Liu JL, et al. Circulating levels of IGF-1 directly regulate bone growth and density. *J Clin Invest*. 2002;110:771–81.
23. Prosser CG. Insulin-like growth factors in milk and mammary gland. *J Mammary Gland Biol Neoplasia*. 1996;1:297–306.
24. Hong H, Cui ZZ, Zhu L, Fu SP, Rossi M, Cui YH, et al. Central IGF1 improves glucose tolerance and insulin sensitivity in mice. *Nutr Diabetes*. 2017;7:2.
25. Kandalla PK, Goldspink G, Butler-Browne G, Mouly V. Mechano Growth Factor E peptide (MGF-E), derived from an isoform of IGF-1, activates human muscle progenitor cells and induce an increase in their fusion potential at different ages. *Mech Ageing Dev*. 2011;132:154–62.
26. Hill M, Wernig A, Goldspink G. Muscle satellite (stem) cell activation during local tissue injury and repair. *J Anat*. 2003;203:89–99.
27. Hill M, Goldspink G. Expression and splicing of the insulin-like growth factor gene in rodent muscle is associated with muscle satellite (stem) cell activation following local tissue damage. *J Physiol*. 2003;549:409–18.
28. Stavropoulos A, Varras M, Philippou A, Vasilakaki T, Varra VK, Varra FN, et al. Immunohistochemical expression of insulin-like growth factor-1Ec in primary endometrial carcinoma: Association with PTEN, p53 and survivin expression. *Oncol Lett*. 2020;20:395.
29. Karagiannis AK, Philippou A, Tseleni-Balafouta S, Zevolis E, Nakouti T, Tsopanomichalou-Gklotsou M, et al. IGF-1Ec expression is associated with advanced differentiated thyroid cancer. *Anticancer Res*. 2019;39:2811–9.
30. Christopoulos PF, Msaouel P, Koutsilieris M. The role of the insulin-like growth factor-1 system in breast cancer. *Mol Cancer*. 2015;14:43.
31. Alexandraki KI, Philippou A, Boutzios G, Theohari E, Koutsilieris M, Kassiani Deladetsima I, et al. IGF-1Ec expression is increased in secondary compared to primary foci in neuroendocrine neoplasms. *Oncotarget*. 2017;8:79003–11.
32. Alagaratnam S, Loizidou M, Yang SY, Fuller B, Ramesh B. Increased expression of IGF-1Ec with increasing colonic polyp dysplasia and colorectal cancer. *J Cancer Res Clin Oncol*. 2020;146:2861–70.

ACKNOWLEDGEMENTS

Part of the work of this study was supported by “The Greek Research Infrastructure for Personalised Medicine (pMED-GR)” (MIS 5002802) which is implemented under the Action “Reinforcement of the Research and Innovation Infrastructure”, funded by the Operational Programme “Competitiveness, Entrepreneurship and Innovation” (NSRF 2014-2020) and co-financed by Greece and the European Union (European Regional Development Fund). We would also like to thank Professors C. Consoulas and C. Palikaras for their useful comments regarding the presentation of the data in the present article.

AUTHOR CONTRIBUTIONS

AA: Study design, designing and obtaining the constructs, generation of tumours into SCID mice, IF, Ab administration, tumour follow-up, cell culture experiments, writing of the paper. NA: In charge of the clinical part of the study, collection of patient material and clinicopathological characteristics of the patients, MS: Cell culture experiments, tumour removal, sentinel node staining, and removal. CP: Patient immunohistochemistry and evaluation. GA: Animal immunohistochemical analysis and evaluation. MS: Proteomics analysis, phosphoproteomics analysis, GP: Proteomics and phosphoproteomics evaluation, EC: Statistical analysis. MK: Contribution to the study design and in the writing of the paper.

FUNDING

This study was financed by the Physiology Laboratory and the National and Kapodestrian University of Athens.

COMPETING INTERESTS

The authors declare no competing interests.

ETHICS APPROVAL AND CONSENT TO PARTICIPATE

A written informed consent (IC) was obtained from all the patients prior to participation in the present study (attached). The study has been approved by the Institutional Ethics Committee and all the experimental procedures conformed to the Declaration of Helsinki (attached).

ADDITIONAL INFORMATION

Supplementary information The online version contains supplementary material available at <https://doi.org/10.1038/s41416-024-02713-8>.

Correspondence and requests for materials should be addressed to Athanasios Armakolas.

Reprints and permission information is available at <http://www.nature.com/reprints>

Publisher's note Springer Nature remains neutral with regard to jurisdictional claims in published maps and institutional affiliations.

Springer Nature or its licensor (e.g. a society or other partner) holds exclusive rights to this article under a publishing agreement with the author(s) or other rightsholder(s); author self-archiving of the accepted manuscript version of this article is solely governed by the terms of such publishing agreement and applicable law.